DTU Library

Hygrothermal assessment of north-facing, cold attic spaces under the eaves with varying structural roof scenarios

Jensen, Nickolaj Feldt; Bjarløv, Søren Peter; Johnston, Christopher Just; Pold, Casper Fabian Hillestrøm; Hjorslev Hansen, Morten; Peuhkuri, Ruut Hannele

Published in:
Journal of Building Physics

Link to article, DOI:
10.1177/1744259119891753

Publication date:
2020

Document Version
Peer reviewed version

Citation (APA):
Jensen, N. F., Bjarløv, S. P., Johnston, C. J., Pold, C. F. H., Hjorslev Hansen, M., & Peuhkuri, R. H. (2020). Hygrothermal assessment of north-facing, cold attic spaces under the eaves with varying structural roof scenarios. *Journal of Building Physics*, *44*(1), 3-36. https://doi.org/10.1177/1744259119891753

Hygrothermal assessment of north facing, cold attic spaces under the eaves with varying structural roof scenarios

Nickolaj Feldt Jensen [a, *], Søren Peter Bjarløv [a], Christopher Just Johnston [a,b], Casper Fabian Hillestrøm Pold [c], Morten Hjorslev Hansen [d], Ruut Hannele Peuhkuri [e],

[a] Department of Civil Engineering, Technical University of Denmark, Brovej 118, 2800 Kgs. Lyngby, Denmark

[b] NIRAS Gruppen A/S, Building and Design, Sortemosevej 19, 3450 Allerød, Denmark

[c] Goritas A/S, Lautrupvang 8, 2750 Ballerup, Denmark

[d] Fonden BYG-ERFA, Ny Kongensgade 13, 1472 Copenhagen K, Denmark

[e] Danish Building Research Institute, Aalborg University, Copenhagen, Denmark

[*]Corresponding author.
E-mail addresses: nicf@byg.dtu.dk (N.F. Jensen), spb@byg.dtu.dk (S.P. Bjarløv), cjjo@niras.dk (C.J. Johnston), chp@goritas.dk (C.F.H. Pold), mhh@byg-erfa.dk (M.H. Hansen), rup@sbi.aau.dk (R.H. Peuhkuri).
Phone: +45 45251803

Funding and acknowledgment

This research project was financially supported by The Landowners' Investment Foundation (GI.dk), which is gratefully acknowledged. We would also like to thank Christian Peter Rasmussen and Lars Kokholm Andersen for developing the physical system and programming between computer and sensors.

ABSTRACT

The objective was to test whether compliance with current Danish best practice recommendations concerning design of the cold attic space will prevent damaging moisture levels. The project was performed as a full-scale experimental setup in the cool temperate climate of Denmark. The setup comprised 18 north facing attic spaces with varying ventilation principles and varying infiltration scenarios. Relative humidity and temperature were measured in attic spaces, indoor and outdoor for almost three years. The hygrothermal performance of the attics was evaluated by post-processing and comparing the data with predicted mould growth risk and with visual observations of mould growth.

The results showed that following the recommended passive ventilation strategies made the hygrothermal performance in attics with diffusion-open roofing underlay worse. Also, increasing vapour diffusion tightness of the roofing underlay made the hygrothermal performance of the cold attic spaces under the eaves worse, except for attics with passive ventilation but without infiltration. The hygrothermal performance of the attics with diffusion-tight roofing underlay was poor when combining infiltration and the assessed ventilation strategy. The performance of the same attic without infiltration showed that some degree of ventilation was needed. External roof insulation did not significantly improve the hygrothermal performance of the attic.

KEYWORDS

Cold attics, ventilation, diffusion-open roofing underlay, insulated roofing underlay, hygrothermal performance, mould growth

Introduction

The objective of this study was to test whether compliance with the current Danish best practice recommendations concerning design of cold attic spaces under the eaves (atticin addition to the requirements in the Danish building regulations 2018 (BR18) (TBST, 2018) regarding airtightness of the building envelope (less than 1.0 l/s per m2 heated floor area at 50 Pa pressure difference) will prevent damaging moisture levels in the attics. Danish guidelines (Brandt et al., 2009, 2013) state: “It cannot be expected that diffusion-open roofing underlay (Z-value < 3 GPa m^2 s/kg) will to a sufficient extent remove moisture from the attic spaces and attic spaces under the eaves (when the floor width > 1 m). Unless the vapour barrier toward the indoor climate is perfectly installed, these attic spaces will need some degree of ventilation.”

In Denmark cold attics are traditionally ventilated with outdoor air to control moisture levels. However, high moisture levels and mould growth are still very common problems despite compliance with Danish guidelines (Bjarløv et al., 2016; Pold, 2015). Other studies document similar tendencies for attics in compliance with best practice guidelines for other geographical locations in cool, temperate climates (Essah et al., 2009; Fugler, 1999; Hagentoft and Kalagasidis, 2014; Harderup and Arfvidsson, 2013; Nik et al., 2012;

Ojanen, 2001; Roppel et al., 2013; Roppel and Lawton, 2014; Uvsløkk, 2005). Detailed statistics concerning moisture damages in attics are lacking in Denmark. However, detailed study of attics in Sweden conducted by Boverket (National Board of Housing, Building and Planning) in 2007 (Boverket, 2009) showed occurrence of high moisture concentration, mould or odours in 15 % of single-family houses, 3 % of multi-story residential buildings, and < 1 % of commercial buildings.

Past research regarding cold ventilated attics has tried to determine failure reasons and thresholds for moisture safe solutions. (Fugler, 1999; Harderup and Arfvidsson, 2013; Holm and Lengsfeld, 2006) investigated the effect of varying ventilation rates and found lowered moisture concentration in the attics with reduced ventilation. (Fugler, 1999; Ge et al., 2018; Hagentoft, Carl-eric; Kalagasidis, 2013; Kalagasidis, 2007) however point out, attic ventilation is required in case of severe infiltration from the conditioned spaces, while (Essah et al., 2009) found reduced moisture levels with attic ventilation. In addition, (Hagentoft and Kalagasidis, 2014; Nik et al., 2012) investigated the performance of different attic designs subjected to possible future climate scenarios. Findings indicate poor performance for naturally ventilated attics with eave-to-eave ventilation, gable-side ventilation, as well as with reduced ventilation.

(Harderup and Arfvidsson, 2013; Ojanen, 2001; Pold, 2015) investigated sealed attic structures with diffusion-open underlay as an alternative to traditional attic ventilation. These indicate diffusion-open underlay reduces moisture concentration in the attic. Correspondingly, (Uvsløkk, 2005) found diffusion-open attics to perform better with decreasing attic ventilation, and improved performance with decreasing diffusion resistance of the underlay. (Bjarløv et al., 2016; Pold, 2015) support results in (Uvsløkk, 2005), indicating increased moisture concentration in ventilated, north oriented cold attics. However, unlike to experimental results in (Bjarløv et al., 2016), Computational Fluid Dynamics (CFD) simulations in (Pold, 2015) indicate ventilation by pressure equalization (top valve only) is worse than single-sided ventilation (with top- and bottom valve). (Essah et al., 2009) found reduced attic condensation with decreasing vapour diffusion resistance of the underlay. Condensation was however not prevented despite a highly diffusion-open underlay (S_d-value = 0.02 m).

In addition, (Fugler, 1999; Hagentoft and Kalagasidis, 2008, 2010; Iffa and Tariku, 2016; Roppel and Lawton, 2014; TenWolde and Rose, 1999) indicate a static ventilation solution may not be suitable for all climates. As climate differs greatly by the geographical location, attic ventilation itself may be a source of moisture in some climates. In this context, investigated sealed attics with sensor controlled mechanical ventilation, to ensure ventilated only when the outdoor air has a drying potential. The solution has shown successful in maintaining safe moisture levels in the attics. Simulation studies (Hagentoft and Kalagasidis, 2014, 2016; Nik et al., 2012) of attics with controlled ventilation correlate with experimental findings.

(Hagentoft and Kalagasidis, 2014; Harderup and Arfvidsson, 2013; Nik et al., 2012) investigated the influence of long-wave radiation. Heat losses due to long-wave radiation is greatest during cold nights with clear skies. Causing the temperature of outermost roofing elements to drop below that of the outdoor air, increasing condensation risk. Studies found external roof insulation reduced condensation risk inside the attic.

Literature review on hygrothermal performance and moisture related problems in cold, ventilated attics suggest findings are not consistently in agreement. Previous studies were structured very diverse with different variations, assumptions and goals in mind, making direct comparisons hard, thus leaving room for further research in this field.

Present paper is the second phase of a two-phase project, of which phase one was reported in (Bjarløv et al., 2016). Relative humidity (RH) and temperature measurements are presented, and the risk of mould growth assessed through visual observation and mathematical modelling.

Phase two differs by investigating the same three ventilation scenarios combined with varying diffusion resistance of the underlay, several infiltration scenarios, including constant airflow by mechanical ventilation, and external roof insulation.

Project significance:

To examine numerous not previously examined parameter variations for north oriented cold attic spaces under the eaves, including all influential factors.

To examine the effect of different infiltration rates (down to 10% of the Danish building code) on the hygrothermal behaviour of cold attic spaces under the eaves with and without passive ventilation.

To examine the effect of external roof insulation, against heat loss due to long-wave radiation, for cold attic spaces under the eaves.

To examine if natural ventilation does occur within the cold attic spaces under the eaves, or if all air in the cavity is primarily passing over the valves without entering the attic space and causing increased infiltration due to lower pressure occurring in the ventilated cavity.

If natural ventilation does occur, how does it perform compared to the mechanical system?

Method

The experimental setup consisted of two 11.5 m insulated containers, both with a 45° single sided pitched roof, oriented towards north. Each roof was constructed with nine equal sized cold attic spaces under the eaves, and a conditioned loft corridor towards south (Figure 1). The container and loft corridor was connected via two hatch openings, and a couple of small fans were installed to create a bit of air flow between the two zones. The size of the experimental attics (with a triangular cross section of 1 m by 1 m) is close to the attics in full-scale buildings. Orientation towards north is considered worst-case scenario compared to similar attics towards other orientations, as the roof receives a limited amount of solar radiation. Results from the examined attics cannot be directly applied full sized pitched roofs, as the ventilation scheme and boundary conditions are different. Full sized pitched roofs are however expected to perform better than the examined attics. The interior of the container served as conditioned indoor environment. The experiment was performed at the test site of the Department of Civil Engineering at DTU (55.79°N, 12.53°E).

Construction

Attics were constructed with special care and attention towards reduction of potential sources of error from unintentional heat, air or moisture transport. Hygric and thermal decoupling were established between individual attics, and interior spaces using a vapour barrier and thick insulation layers. The attics were constructed according to best practice directive to obtain an airtightness below 1.0 l/s per m2 at 50 Pa pressure difference (including measures such as taping vapour barrier overlaps). Blowerdoor test was not practically possible for this setup. Therefore special attention was paid on the craftman work quality during the construction of the experimental setup to such extend that the airtightness would be according to the directive. The attics had the interior dimensions (LxWxH) 1.25 m x 1 m x 1 m. The indoor climate was heated to 20 °C with 60 % RH (equal to a water vapour content of 10 g/m^3) using humidifiers and electrical convectors. The RH of the indoor climate corresponds to the upper boundary of highest humidity class for dwellings (humidity class 3) (DS/EN ISO 13788, 2013). Humidity class 3 (unknown residence density) is equivalent to a moisture excess of 4-6 g/m^3, while humidity class 2 (normal residence density) is 2-4 g/m^3. Moreover, the containers were fitted with a valve in each end, dimension to provide an approximate air change rate of 0.5 h^{-1} as required for normal residential buildings (TBST, 2018). The high indoor humidity was chosen in order to test the design under a worst case scenario.

[insert Figure 1.]

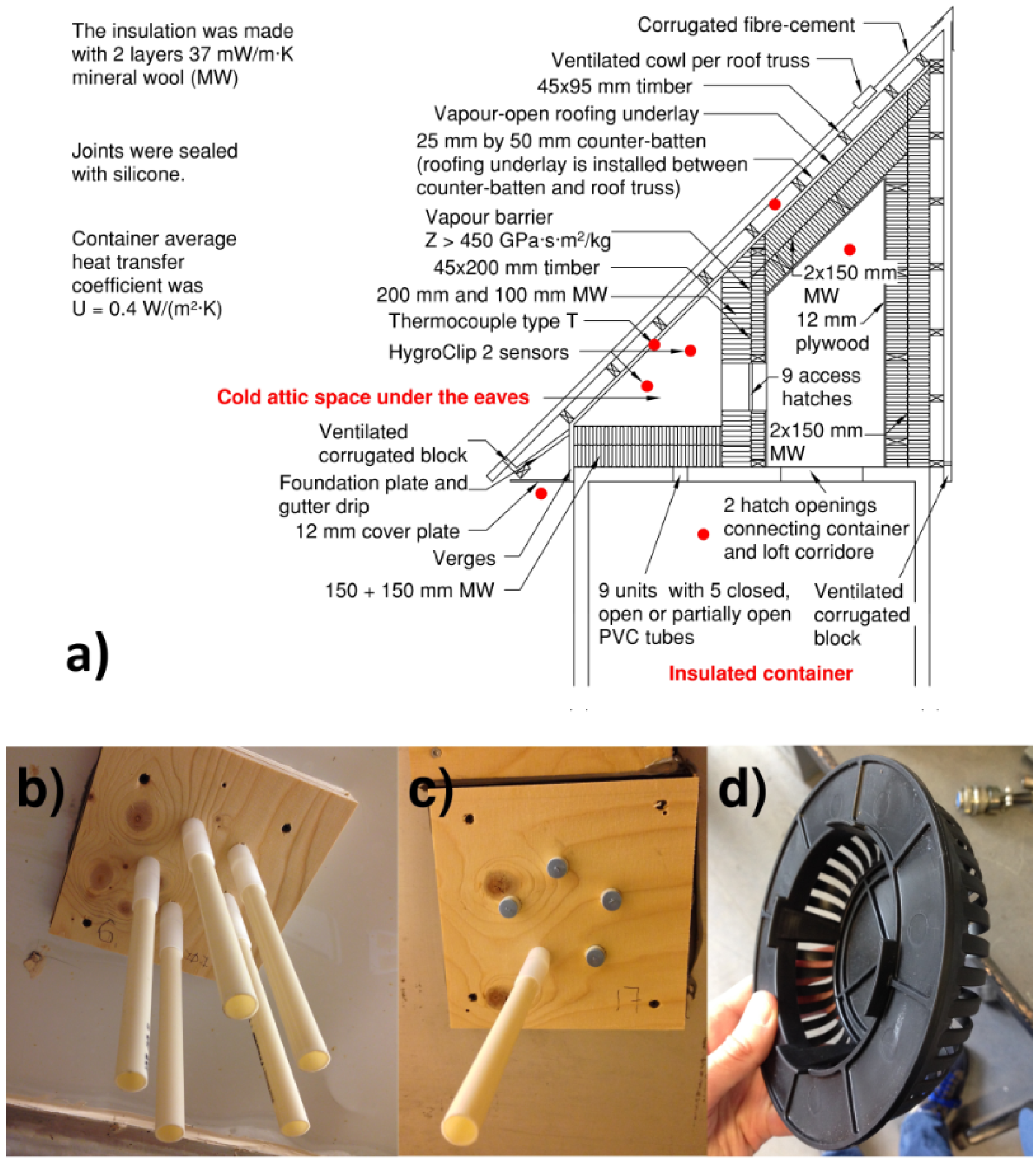

Figure 1 a) Vertical section of the attic setup. Red dots indicate sensor locations. b) 100% infiltration through 5 open PVC tubes. c) 20% infiltration through 1 open PVC tube. d) Ventilation valve installed in the underlay.

Physical phenomena

Several moisture flows were considered in the experimental setup, see Figure 2a:
Where

$G_{v,cont.vent\ north/south}$: vapour flow from fresh air valves, installed in the container walls to prevent the occurrence of negative pressure within the containers.

$G_{v,inf}$: vapour flow from PVC tubes connecting attics and indoor environment allowing infiltration to occur.

$G_{v,\ in/out}$: vapour flow from ventilation valves installed in the underlay allowing for ventilation of the attics with outdoor air. The experimental setup was limited to ventilation from only one side of the roof structure.

$G_{v,roof.underlay}$: vapour flow through the underlay.

$G_{v,roof.cav\ mid/top}$: vapour flow in outdoor air in the cavity passing over the attics instead of entering through the valves.

$G_{v,eave}$: vapour flow in outdoor air entering the cavity at the eave.

$G_{v,cowl}$: vapour flow in outdoor air and infiltration air exiting the cavity at the roof cowl.

The $\mathbf{G}_a$ variables in Figure 2b-c represent the difference air flows influencing the attic spaces, which are dealt with in later sections – determining the infiltration- and ventilation flows.

Variables $\mathbf{G}_{v,inf}$, $\mathbf{G}_{v,in/out}$, and $\mathbf{G}_{v,roof.underlay}$ were altered, and are further described in section under parameter variations. Heat loss from long-wave radiation, $Q_{long\text{-}wave}$ was also considered as the cooling effect on the roof structure increases condensation risk within the attics.

Mechanical ventilation was installed in two attics to test whether ventilation would occur within the attics due to natural airflows, where the outdoor air enters the attic through the lower valve and exits through the upper valve (Figure 2b). Alternatively, if the outdoor air entering the cavity would simply pass through without entering the attic itself, this would cause a situation with no natural ventilation occurring within the attic and increased infiltration (Figure 2c).

[insert Figure 2.]

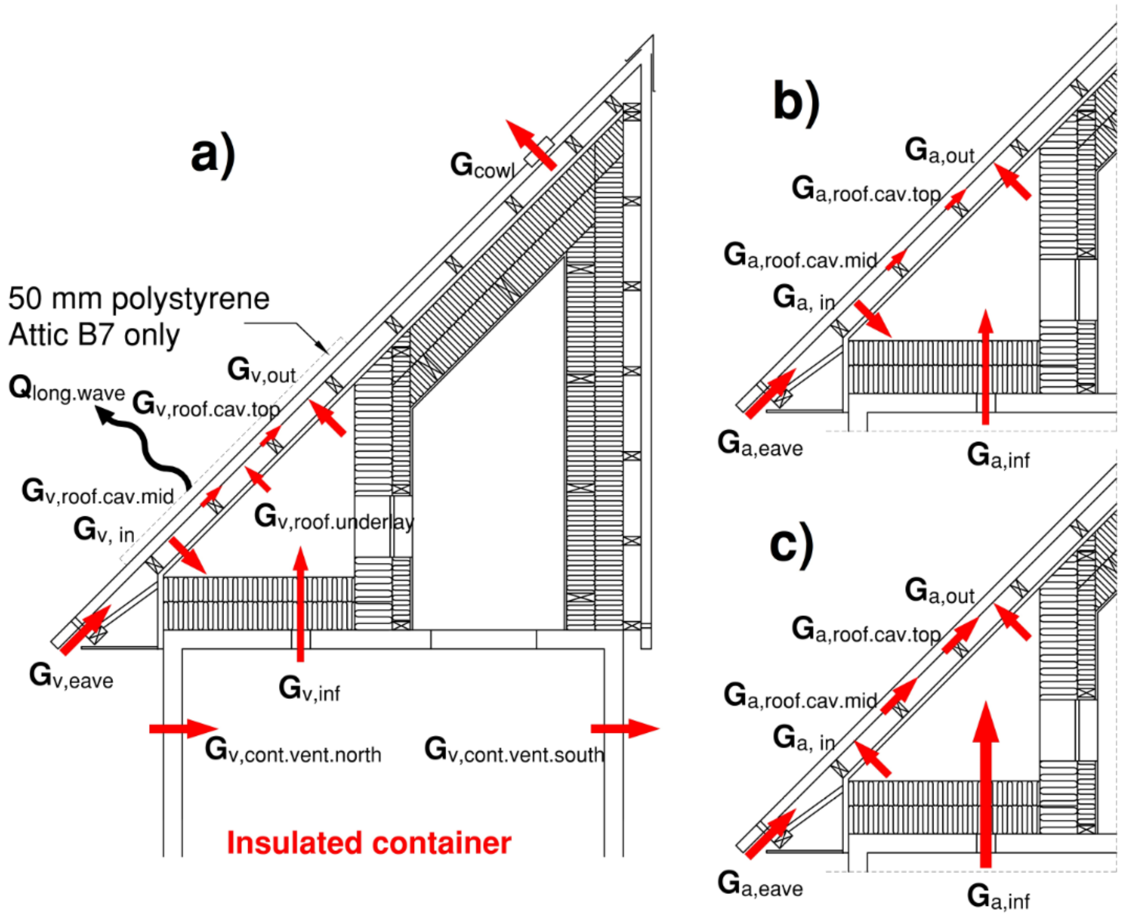

Figure 2 a) Physical phenomena considered in the attic setup. b) Natural ventilation scenarios one: in and out flows of outdoor air. c) Natural ventilation scenarios two: low pressure in the cavity.

Parameter variations

The experimental setup consisted of 18 cold attics, each with a different set of parameter variations, representing different structural roof scenarios (Table 1). The setup permitted to examine the effect of changes in three series of variables. First series was the underlay, where three different types were investigated: 1) Tyvek Pro (diffusion-open), Z-value = 0.1 GPa·s·m^2/kg. 2) Monarperm 1000 (diffusion-open), with Z-value = 1.0 GPa·s·m^2/kg. 3) Monarfol Super (diffusion-tight), with Z-value = 855 GPa·s·m^2/kg. Monarperm 1000 was included as a reference to phase one (Bjarløv et al., 2016). Motivation for different underlays was to investigate the influence of the underlay vapour permeability on the hygrothermal conditions in the attics under different ventilation scenarios. Diffusion-tight attics were included as a reference for the diffusion-open attics, not to assess the performance of diffusion-tight attics.
Second series of parameter variations was the infiltration rate between indoor environment and attics. The attics were sealed against unintentional infiltration between

individual attics and the interior environment. However, real attic structures do experience some infiltration from the adjacent conditioned spaces. The experiment setup was designed to emulate infiltration concentrated around the wall-to-ceiling junction. While still valid within the framework of the local building code, worst-case scenario was assumed. Attics were connected to the indoor environment using five closed, open or partly open PVC tubes (internal diameter 10-13.3 mm), penetrating the attic floor, to emulate the effect of infiltration. Four infiltration scenarios were investigated: 1) no infiltration from the indoor environment. 2) 3.4 l/s at 50 Pa (100 % infiltration). 3) 0.34 l/s at 50 Pa (10 % infiltration). 4) 0.68 l/s at 50 Pa (20 % infiltration). See Table 1. The infiltration rate per attic of 3.4 l/s at 50 Pa correspond to an infiltration rate of 1.0 l/s m^2 heated floor area of the container at 50 Pa through the building envelope, thus complying with Danish building regulations 2018.

Third series of parameter variations was ventilation strategy. Above-mentioned variations were combined with one of four ventilation scenarios, to investigate the significance of underlay and infiltration rate in relation to the individual ventilation strategy, see Table 1. Following ventilation scenarios were investigated: 1) Unventilated (UV), with no ventilation valve. 2) Pressure equalization (PE), with one ventilation valve located in top corner of the underlay. 3) Single-sided ventilation (SSV), with two ventilation valves located diagonally in the top and bottom corners of the underlay. 4) Mechanical ventilation (MV), with two ventilation fans located diagonally in the top and bottom corners of the underlay. The bottom fan functioning as inlet fan, and the top fan as extraction fan, providing a constant flow rate of 0.22 l/s, corresponding to an air change rate (ACH) of approximately 1.27 h^{-1}. Mechanical ventilation was installed with balanced ventilation to minimize influence on the infiltration from the conditioned spaces. Mechanical ventilation was installed on June 29th of 2015, and prior to installation the attics were fitted with SSV. The ventilation valves for the natural ventilation had a flow area of 50 cm^2.

A single attic was fitted with external roofing insulation of 50 mm polystyrene, to investigate the significance of long-wave radiation. (Table 1).

Table 1 Overview of the attic variations. [1] Fitted with exterior insulation. Ventilation strategies: unventilated (UN), pressure equalization (PE), single-sided ventilation (SSV), and mechanical ventilation (MV). 100 % infiltration corresponding to 3.4 l/s at 50 Pa.

Attic	Underlay diffusion resistance [GPa·s·m^2/kg]	Infiltration [%]	Ventilation strategy [-]
A1	855	0	SSV
A2	855	100	UN
A3	855	100	SSV
A4	855	10	UN

A5	855	10	SSV
A6	855	20	UN
A7	855	20	SSV
A8	855	20	MV
A9	855	100	MV
B1	0.1	0	UN
B2	0.1	0	PE
B3	0.1	0	SSV
B4	0.1	100	UN
B5	0.1	100	PE
B6	0.1	100	SSV
B7[1]	0.1	100	UN
B8	1.0	100	SSV
B9	855	0	UN

Measurement equipment

Temperature and RH were measured in attics, containers, loft corridors, underlay above each attic, ventilated cavity, and outside of the containers throughout the experimental period. Measurements were logged every 10 minutes. Two sensors were installed in each attic and measurements for temperature and RH were averaged for each time step. Three types of measurement equipment were used in the experiment: 1) Rotronic HygroClip 2 S, measuring temperature and RH. 2) Thermocouple Type T, measuring temperature. 3) Sensirion SDP1000-L025 pressure sensors (Sensirion, 2013) installed on both sides of the infiltration tubes for attics A5, A7, B5 and B6. The pressure was measured just off the tubes, so the measurement should corresponds to the pressure that the tubes "experience" at each end. Output was an electrical analogue signal, converted into pressure difference using:

$$\Delta p_{a,tube} = 62\ Pa \cdot (U - 2.1\ \mathrm{V})/1.9\ \mathrm{V} \qquad (1)$$

Where $\Delta p_{a,tube}$ is the pressure difference across the tube [Pa] and U the measured output voltage [V]. Resulting pressure difference was multiplied with an altitude correction factor (Table 3 in (Sensirion, 2013), 0.955 for an altitude of 40 m) and a correction factor for connection hose length (Figure 7 in (Sensirion, 2013), -0.64 % for a length of 0.8 m). Sensors were installed in June 2015. Pressure measurements are available in (Jensen et al., 2019).

Infiltration flow

An approximation of the infiltration flow was calculated from the Sensirion pressure measurements. During the design of the experimental setup, the length and internal dimension of the infiltration tubes were determined through reverse calculation using the maximum allowed infiltration flow (1.0 l/s m^2 at 50 Pa) and the pressure difference across the tubes (50 Pa). The following equations were used:

Local losses:

$$\Delta p_{a,loc} = \Delta p_{a,loc,ent} + \Delta p_{a,loc,exit} = \xi_{ent} \cdot \frac{1}{2 \cdot \rho_a} \cdot \left(\frac{G_a}{A}\right)^2 + \xi_{exit} \cdot \frac{1}{2 \cdot \rho_a} \cdot \left(\frac{G_a}{A}\right)^2 \quad (2)$$

Reynolds number (Re):

$$Re = \frac{v \cdot d_h}{v_a} \quad (3)$$

Friction factor:

Re < 2300 --> $f = \frac{64}{Re}$ (4)

Re > 2300 --> $\frac{1}{\sqrt{f}} = -2 \cdot log\left(\frac{\varepsilon}{3.7 \cdot d_h} + \frac{2.51}{Re \cdot \sqrt{f}}\right)$ (5)

Friction loss:

$$\Delta p_{a,fric} = \frac{f \cdot L}{2 \cdot d_h \cdot \rho_a} \cdot \left(\frac{G_a}{A}\right)^2 \quad (6)$$

Total pressure loss over the tube:

$$\Delta p_{a,tube} = \Delta p_{a,loc} + \Delta p_{a,fric} = \xi_{ent} \cdot \frac{1}{2 \cdot \rho_a} \cdot \left(\frac{G_a}{A}\right)^2 + \xi_{exit} \cdot \frac{1}{2 \cdot \rho_a} \cdot \left(\frac{G_a}{A}\right)^2 + \frac{f \cdot L}{2 \cdot d_h \cdot \rho_a} \cdot \left(\frac{G_a}{A}\right)^2 \quad (7)$$

Where

$\Delta p_{a,loc}$, $\Delta p_{a,loc,ent}$, $\Delta p_{a,loc,exit}$, $\Delta p_{a,fric}$ and $\Delta p_{a,tube}$ pressure losses: total local, local at tube entry, local at tube exit, friction through the length of the tube, and total over the tube [Pa]

ξ_{ent} and ξ_{exit}: local loss factors for tube entry and exit [-], 0.5 and 1.0 respectively

ρ_a: density of air [kg/m^3]

G_a: mass flow rate of air infiltration [kg/s]

A: flow area [m^2], 0.00008 and 0.00014 m^2 respectively for 10 and 13.3 mm tubes

v: air velocity [m/s], 4.90 and 4.81 m/s respectively for 10 and 13.3 mm tubes

d_h: hydraulic diameter of the infiltration tubes [m], 0.01 and 0.0133 m

v_a: kinematic viscosity of air [m^2/s]

f: friction factor [-]

ε: tube roughness [m], 0.0000015 m (glass/plastic)

L: tube length [m], 0.5 and 0.7 m respectively for 10 and 13.3 mm tubes

After determining the length and internal dimensions of the infiltration tubes, calculations were carried out for multiple sizes of infiltration flow to determine the resulting pressure loss over the tubes. The derived pressure losses were plotted against the different sizes of infiltration flow, and polynomial trendlines were used to obtain the relation between pressure loss over the tube and infiltration flow. With the relation between pressure loss over the tube and infiltration flow, it was possible from the pressure measurements to determine an approximation of the infiltration flow for attics A5, A6, B5 and B6. Note that this calculation procedure was performed for each of the three infiltration scenarios: 100, 20, and 10% infiltration. The polynomial trendlines and flow relation are available in (Jensen et al., 2019).

Location and accuracy of measurement equipment are presented in Table 2. Measurement period was July 2014 to May 2017.

Table 2 Location and accuracy of measurement equipment, red dots on Figure 1. Plus sign indicate location of equipment, and multiple plus signs means more sensors.

Instrument	Attic	Container (indoor)	Loft corridor	Underlay	Ventilated cavity	Outdoor
Rotronic HygroClip 2 S	++	+	+		+	+
Thermocouple Type T		+		+		
Sensirion SDP1000-L025	+	+				

Instrument	Measurement	Accuracy	Range
Rotronic HygroClip 2 S	Temperature	± 0.1 K at 23 °C and 10, 35 and 80 % RH	-50 to 100 °C
	RH	± 0.8 % at 23 °C and 10, 35 and 80 % RH	1 to 100 %
Thermocouple Type T	Temperature	± 0.5 K at 0 °C	-200 to 350 °C
Sensirion SDP1000-L025	Pressure difference	0.5 % of full scale / 1.5 % of measured value	-62 to 62 Pa

Tracer gas experiment

Tracer gas measurements were performed for attics A5, A6, B5 and B6 on July 22nd 2015, a day with no rain and mild wind of 1.5 m/s. A constant concentration of Freon 134a gas was maintained inside the indoor environment while simultaneously monitoring the attic concentration caused by infiltration air. Concentrations were measured using an INNOVA 1312 photoacoustic multi-gas monitor (LumaSense Technologies, 2004) for 45-60 minutes after reaching steady state indoors. Variation in measurement period was related to two considerations: 1) Obtaining enough data points to determine an accurate infiltration rate. 2) Avoid changes in boundary conditions disrupting the steady state conditions. Tracer gas measurements are available in (Jensen et al., 2019).

Airflow

Approximations of the airflows in attics A5, A7, B5 and B6 were determined using the pressure differences and tracer gas measurements. For tracer gas experiments maintaining a constant concentration in the indoor environment while monitoring resulting concentration in the attic, airflow into the attics may be determined using:

$$G_{a,in} = \frac{Q_{a,inf} \cdot \rho_{a,in} \cdot \left(\frac{C_{g,inf}}{C_{g,att}} - \frac{\rho_{a,inf}}{\rho_{a,att}}\right)}{\left(\frac{\rho_{a,in}}{\rho_{a,att}} - \frac{C_{g,in}}{C_{g,att}}\right)} \tag{8}$$

Where

$G_{a,in}$: mass flow rate of air entering the attic [kg/s]

$Q_{a,inf}$: volume flow rate of infiltration air [m^3/s]

$P_{a,att}$, $\rho_{a,inf}$, and $\rho_{a,in}$: density of attic, indoor and outdoor air respectively [kg/m^3].

$C_{g,att}$, $C_{g,inf}$, and $C_{g,in}$: average concentrations of Freon gas in attic, indoor and outdoor air respectively [ppm]. $C_{g,in}$ assumed 0.

Equation 8 used to obtain the mass flow rate of air into the attic space, $G_{a,in}$ was derived from the mass balance for tracer gas and the mass balance for air for an attic space considering the ventilation scenario presented in Figure 2b, (Jensen et al., 2019).
Above method was based on following assumptions:
Infiltration flow rate is available from pressure measurements.
All unintentional leakages were neglected.

Mould growth

The mould growth risk was assessed using the mathematical model by Hukka and Viitanen (VTT model) (Hukka and Viitanen, 1999; Ojanen et al., 2010; Viitanen et al., 2015). Critical RH, RHcrit, is calculated as a function of temperature, and mould growth occurs when RH ≥ RHcrit and T > 0 °C. Decline occurs if conditions are not met. Model output is the mould index M that ranges from 0 to 6, corresponding to no growth and

heavy growth (100 % coverage). Values 3-6 are in the visual range. Mould predictions were performed using material class "sensitive", corresponding to wood.
(Brischke and Thelandersson, 2014; Gradeci, Labonnote, Köhler, et al., 2017; Gradeci, Labonnote, Time, et al., 2017) addressed available mould models including governing factors, interrelations, methodology, substrate, extensiveness, rating scale, experimental set-ups for model validation, and (Brischke and Thelandersson, 2014; Gradeci, Labonnote, Köhler, et al., 2017; Gradeci, Labonnote, Time, et al., 2017; Hukka and Viitanen, 1999; Isaksson et al., 2010; Møller et al., 2017; Ojanen et al., 2007; Viitanen et al., 2015) reliability. Findings indicated that models cannot precisely predict the growth, but rather determine the likelihood of mould occurrence. For this study, the mould model was used for relative comparison between design scenarios.
The attics were opened on January 16th, 2018, after 3 years and 6 months of operation, and the extent of the mould infestation observed. Growth was ranked between 1 and 5, based on visual inspection, corresponding to no visual growth and heavy growth.

Results

This section presents measured temperature and RH, derived moisture concentration, and calculated and observed mould growth in the attics. Supplementary plots, summary of key results and datasets are available in (Jensen et al., 2019). The results are shown in different graphs: relative humidity, moisture concentration and VTT mould index (Hukka and Viitanen, 1999; Ojanen et al., 2010; Viitanen et al., 2015). In this way it is possible to find the largest deviations of the results from the different attic variations. The relative humidity and the mould index results are following the same tendencies. In several cases the mould index shows the differences more clearly than the relative humidity and the moisture concentration and gives a better description of the hygrothermal performance since the mould index also include temperature and time. The moisture concentration is presented to document that even small differences in some cases result in larger deviations in the relative humidity and the risk of mould growth.

Measurement results

Results are shown as 15-days (seven days before and after) moving average. Temperature differences related to the effect of external roof insulation is however based on the logged data (Figure 11), and mould calculations on hourly average values. Due to sensor errors four periods of 5-14 days with missing data occurred during the experiment. Three of these periods within the first three months and the last period in late January of 2016. All missing data were interpolated.
The abbreviations state the container name followed by the attic number e.g. A1. The parenthesis following the attic abbreviations specify the following: underlay Z-value/infiltration/ventilation strategy (unventilated, UV; pressure equalization, PE, Single-sided ventilation, SSV).

Effect of diffusion tightness of the roofing underlay

This section investigates the effect of diffusion tightness of the underlay, without infiltration, in a series of attics with increasing flow of outdoor air, by comparing diffusion-open and diffusion-tight attics, with different ventilation strategies. Figure 3 shows:

- More critical relative humidity levels in attics with diffusion-tight underlay (A1, B9) compared to diffusion-open (B1, B3). This is also seen when looking at the mould risk in Figure 13.
- Figure 4 shows similar temperatures in all attics, except for summer periods, where ventilated attics (B2-3, A1) are slightly warmer than unventilated (B1, B9).
- Lowest relative humidity was found in unventilated diffusion-open attic with no infiltration (B1).

[insert Figure 3.]

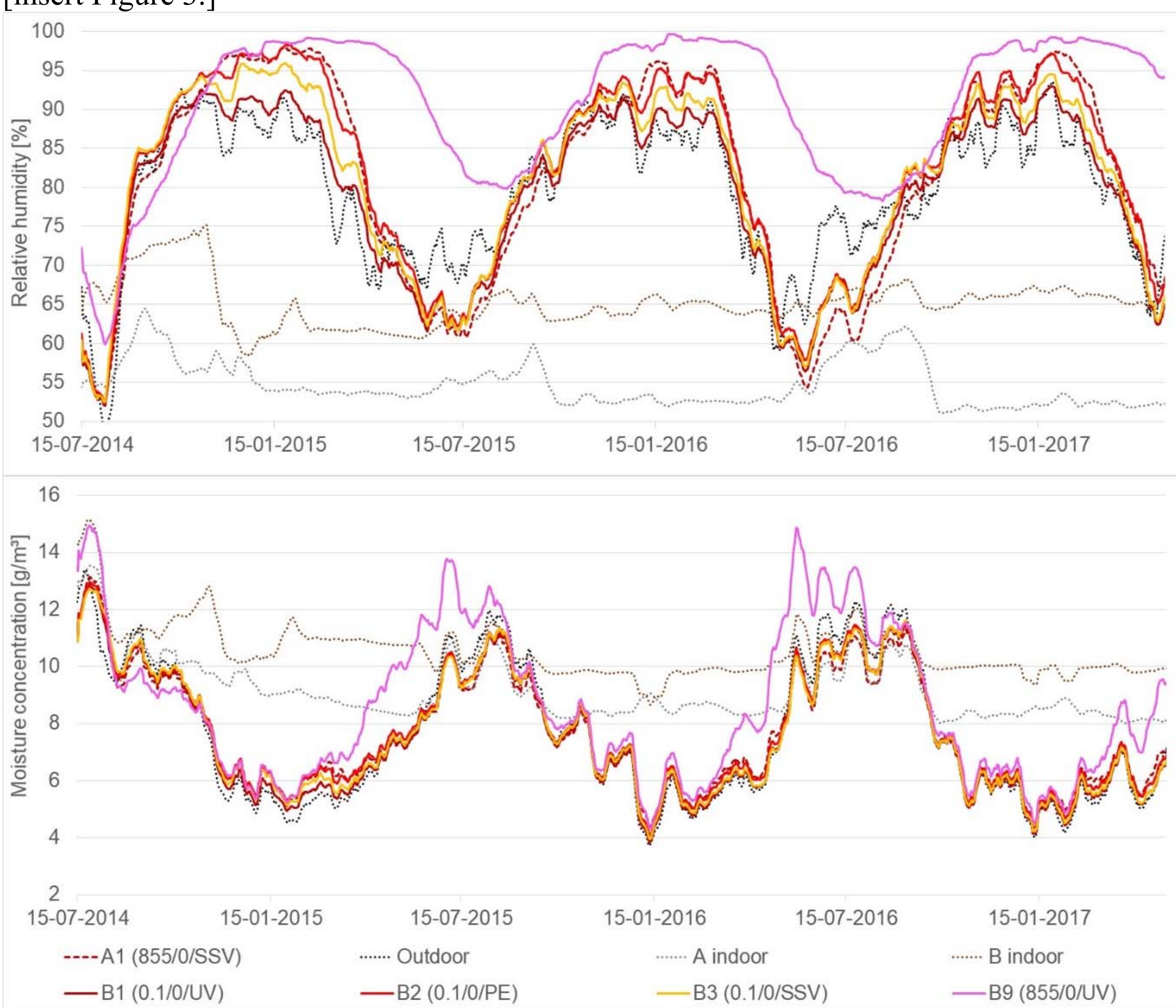

Figure 3 RH (a) and moisture concentration (b) in diffusion-open and -tight attics without infiltration, with and without ventilation.

[insert Figure 4.]

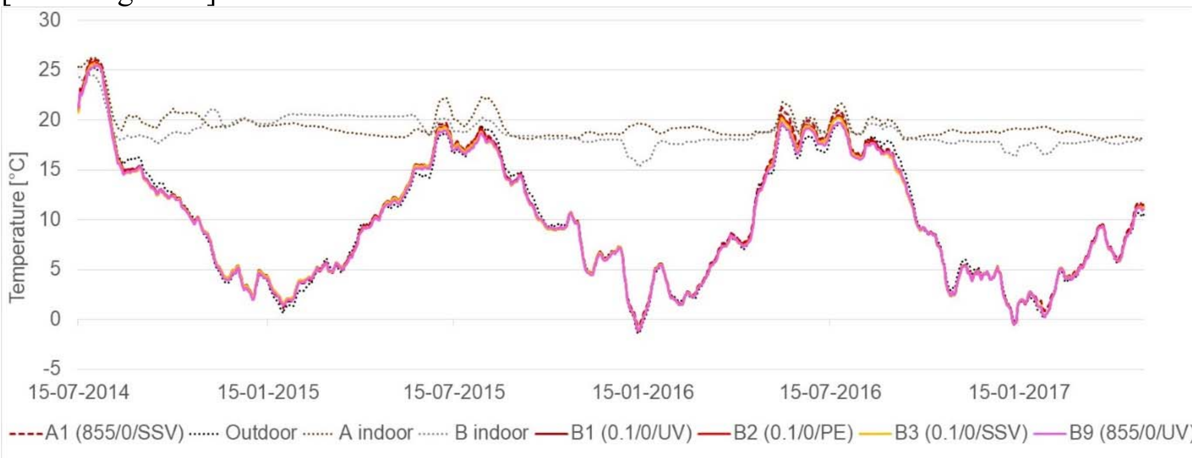

Figure 4 Temperature in diffusion-open and -tight attics without infiltration, with and without ventilation.

Effect of infiltration in a series of attics with diffusion-tight roofing underlay

This section investigates the effect of infiltration in a series of diffusion-tight attics with and without ventilation. Figure 5:

- Increasing the infiltration lowers the relative humidity levels in diffusion-tight unventilated attics (B9, A2), while this increases the levels in diffusion-tight SSV attics (A1, A3).
- SSV increases the relative humidity levels slightly during winter in attics with infiltration (A2, A3). Meanwhile in spring and summer the relative humidity levels are reduced.
- In attics without infiltration (B9, A1), SSV lowers the relative humidity levels throughout the experimental period.

[insert Figure 5.]

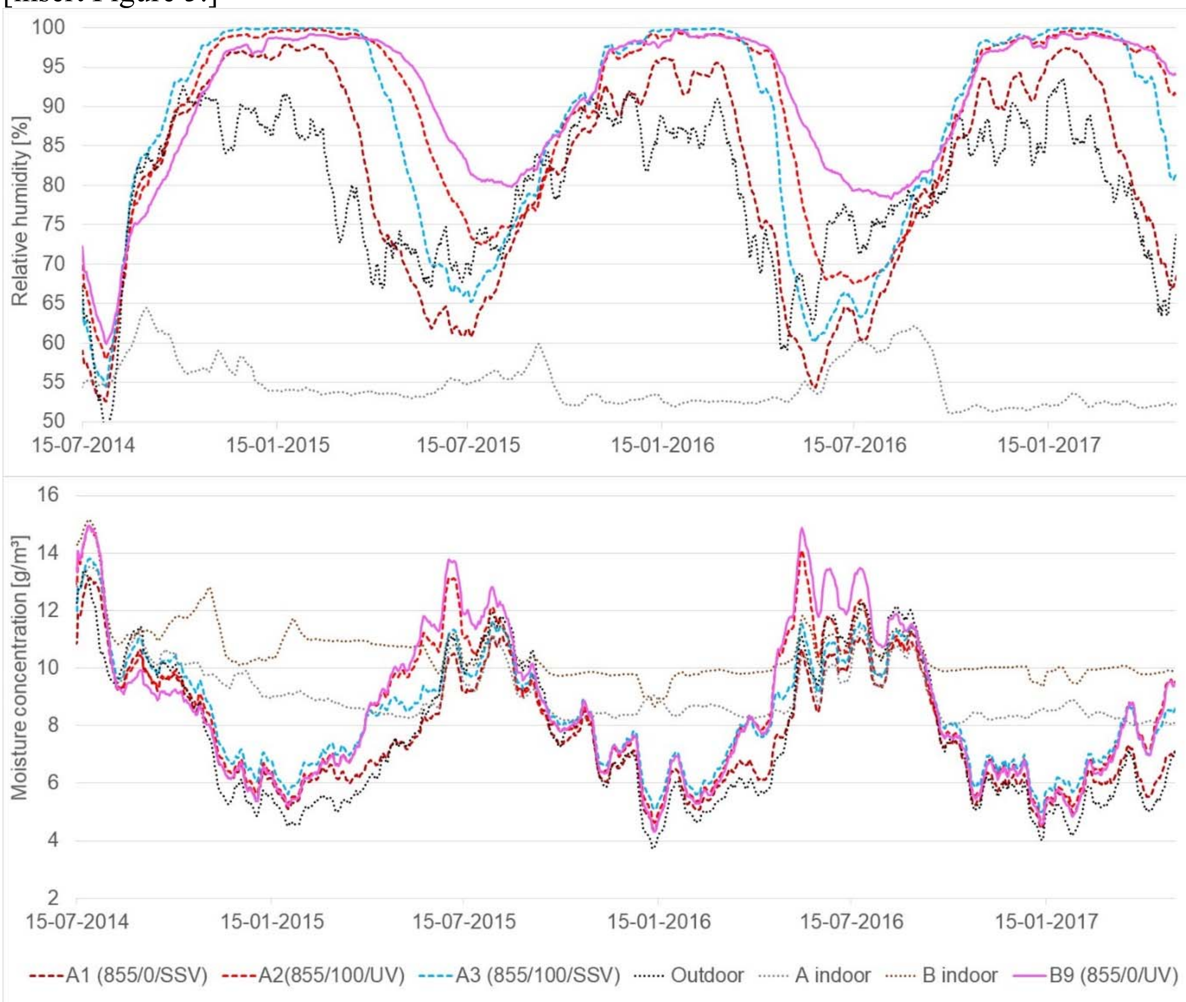

Figure 5 RH (a) and moisture concentration (b) in diffusion-tight attics, with and without infiltration and ventilation.

Effect of infiltration in a series of attics with diffusion-open roofing underlay

This section investigates the effect of infiltration in a series of diffusion-open attics with and without ventilation. Figure 6 shows:

- Increased moisture levels during winter and spring in the diffusion-open attics due to infiltration from the indoor environment (B1 vs B4, B2 vs B5, B3 vs B6), and due to implementation of PE and SSV (B1 vs B2-3, B4 vs B5-6).
- Minor differences were observed during the summer period.
- A combination of infiltration and PE/SSV increases the levels even further (B1 vs B4 vs B5-6).
- The tendencies are also visible for the mould risk in Figure 13.

[insert Figure 6.]

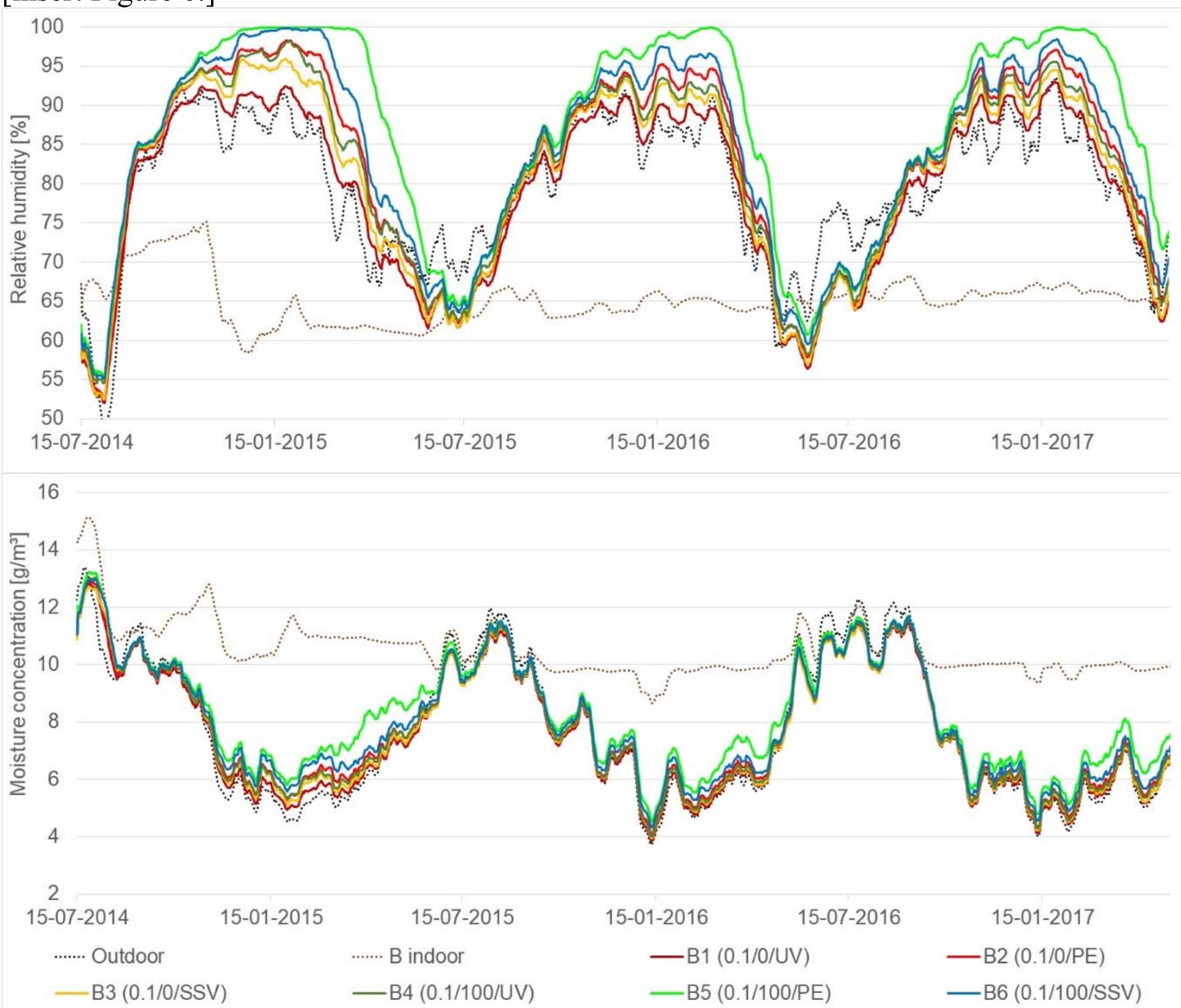

Figure 6 RH (a) and moisture concentration (b) in diffusion-open attics with and without infiltration and ventilation.

.

Effect of infiltration and ventilation

This section investigates the effect of infiltration rates in diffusion-tight attics without ventilation or with SSV ventilation subjected to 0.0, 0.34, 0.68 and 3.4 l/s at 50 Pa, corresponding to 0, 10, 20 and 100 % of the maximum allowed infiltration. Figure 7:.

- Increased infiltration lowers the relative humidity levels in the unventilated diffusion-tight attics during summer, while a small increase is seen during winter.
- The moisture concentration decrease during summer with increasing infiltration, while almost no change was seen during winter.

Figure 8:

- Increased infiltration increases the relative humidity and moisture concentration in diffusion-tight SSV attics throughout the period.

[insert Figure 7.]

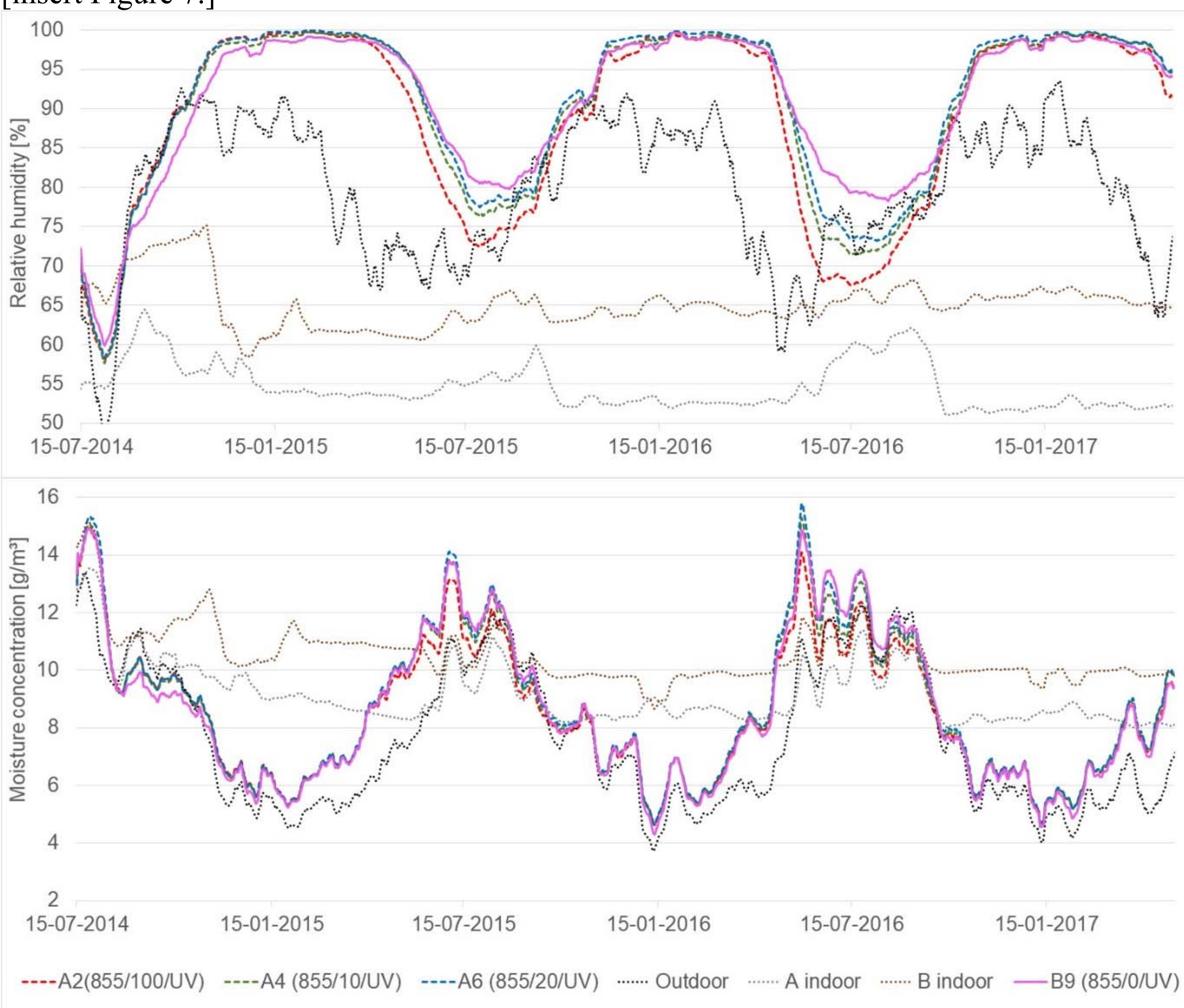

Figure 7 RH (a) and moisture concentration (b) in unventilated diffusion-tight attics with increasing infiltration.

[insert Figure 8.]

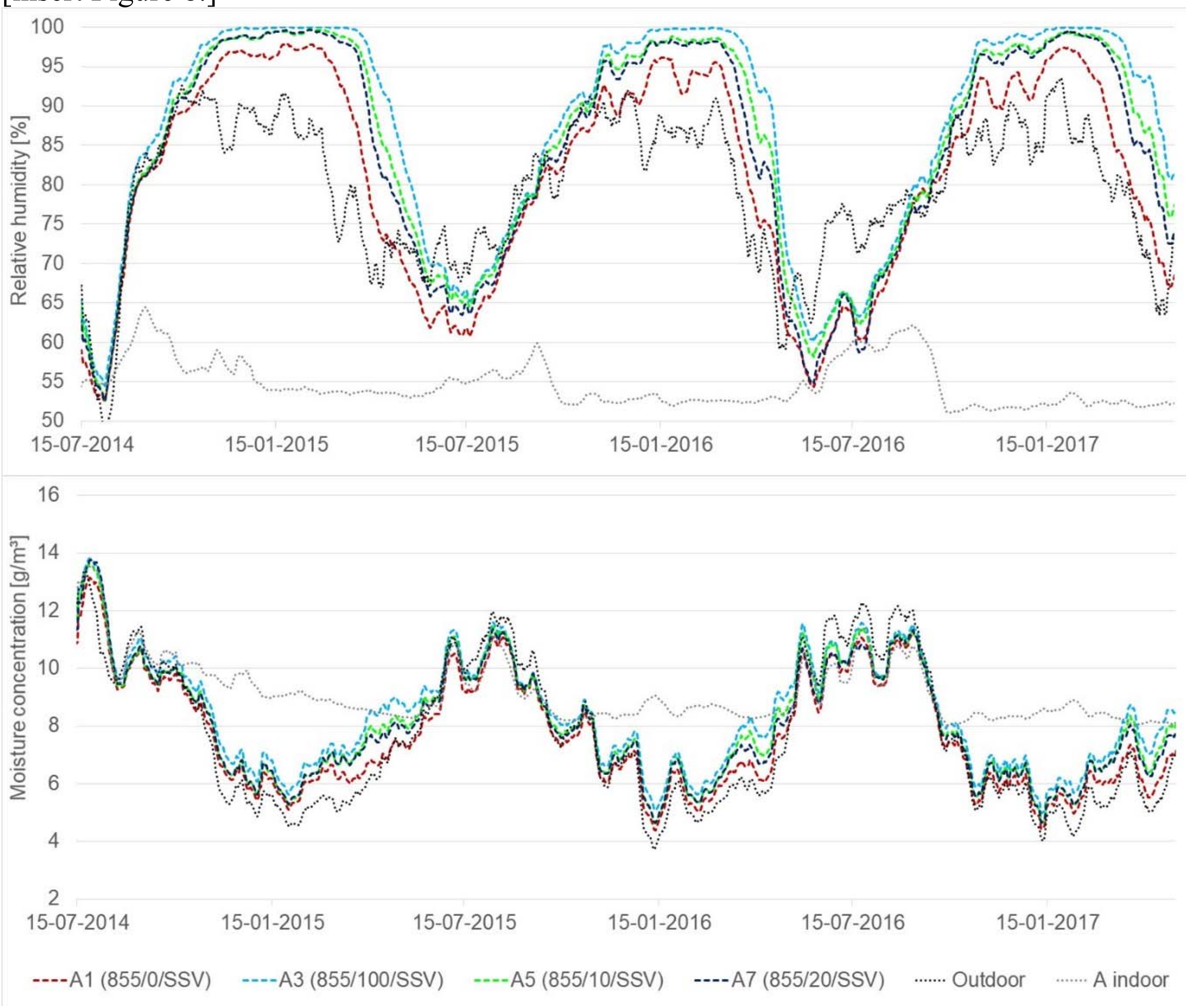

Figure 8 RH (a) and moisture concentration (b) in diffusion-tight SSV attics with increasing infiltration.

Effect of mechanical ventilation at varying infiltration rates

This section investigates if natural ventilation does occur within the attics as described in the section "Physical phenomena". By fitting two diffusion-tight attics (varying infiltration rates) with mechanical ventilation (MV) providing a constant ACH of 1.27 h^{-1}. Results were compared with naturally ventilated SSV attics where the ventilation phenomena were uncertain. Mechanical ventilation was installed on 29.06.2015.

Figure 9 shows:

- Slightly increased moisture levels are seen in the MV attic throughout the experimental period compared to the SSV attic.
- The unventilated attic show the highest relative humidity and moisture concentration in summer, and lowest in winter.
- Similar tendencies are seen in attics with 20 % infiltration (A6-A8). However the deviation between the unventilated (A6) and ventilated (A7-8) attics increases during summer. See supplementary plots.

[insert Figure 9.]

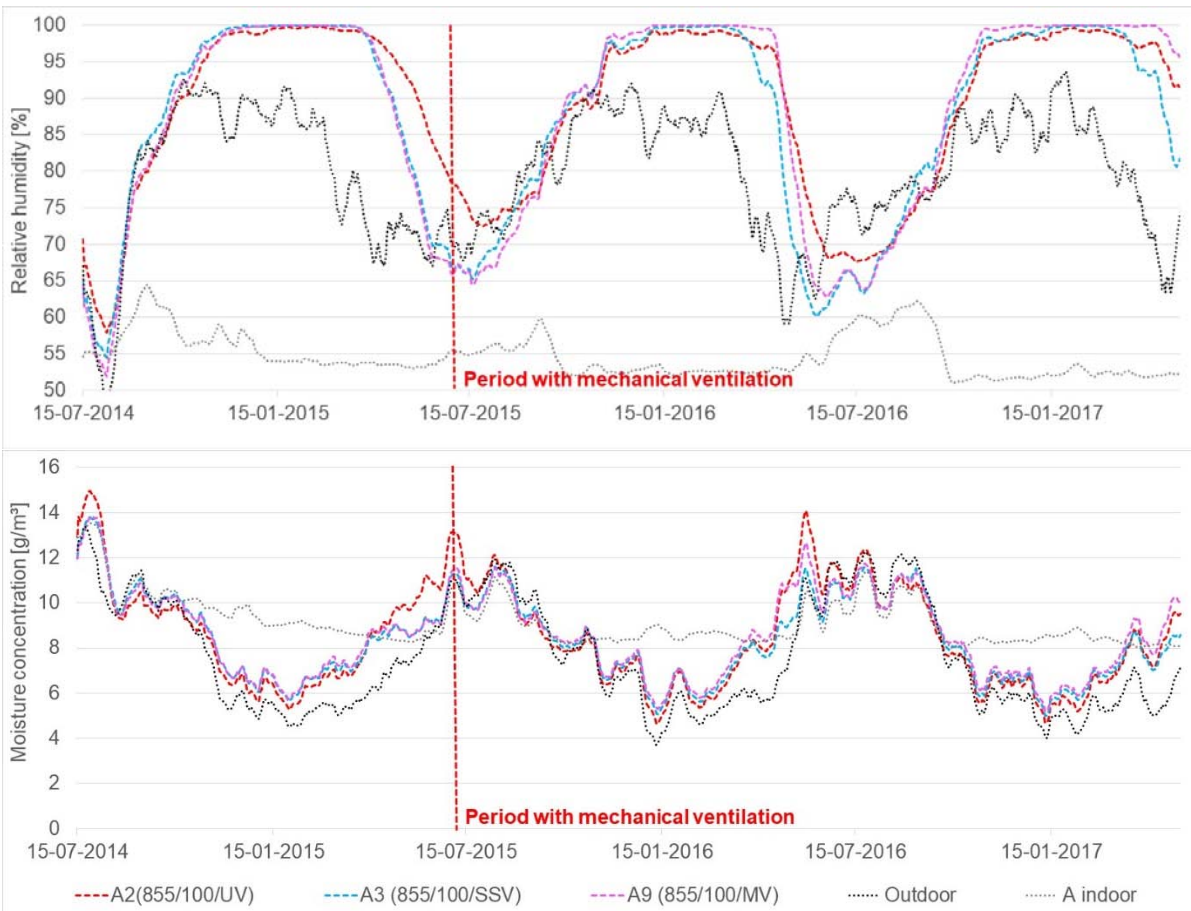

Figure 9 RH (a) and moisture concentration (b) in diffusion-tight attics with increasing infiltration, comparing unventilated, SSV, and MV.

Figure 10 presents the temperatures in SSV, MV or unventilated diffusion-tight attics with 100% infiltration during the last summer (Figure 10a) and winter (Figure 10b) period. Figure 10 show:

- Lowest temperatures during winter in the unventilated attic, and the highest temperatures in the MV attic.
- During summer all the attics are rather alike.
- Similar tendencies in attics with 20 % infiltration.

More temperature plots are available in (Jensen et al., 2019).

[insert Figure 10.]

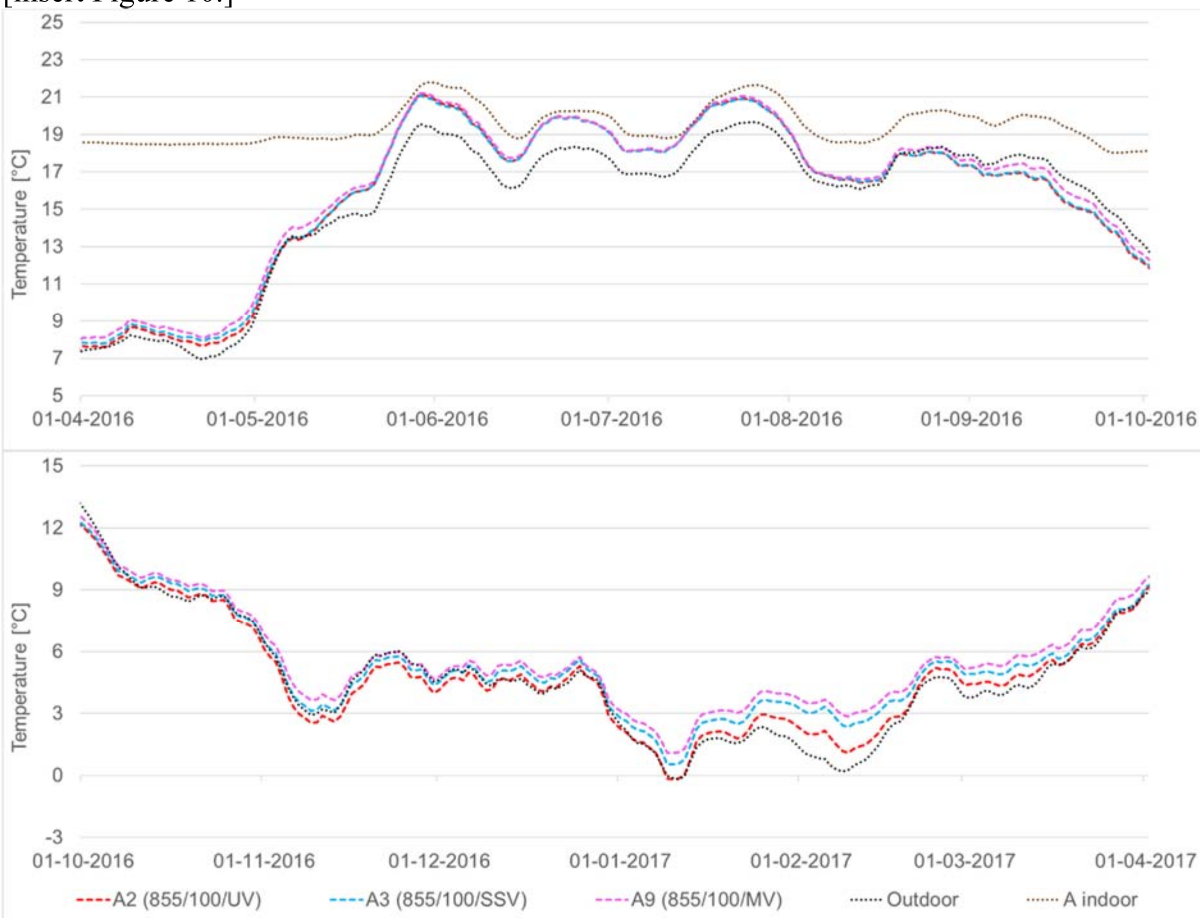

Figure 10 Temperatures during last summer (a) and winter (b) period in the diffusion-tight attics with 100 % infiltration and fitted with SSV, MV or unventilated.

Effect of exterior roof insulation

This section investigates the effect of exterior roof insulation for an unventilated diffusion-open attic with infiltration, to determine the influence of long-wave radiation. Focus is on the cold periods, as heat loss due to long-wave radiation is largest during cold nights with clear skies. The presented data set for temperature is based on the logged measurements per every 10 minutes.

Figure 11 compare temperatures measured in underlays with and without exterior roof insulation during the last summer (Figure 11a) and winter (Figure 11b) period. Figure 11 show:

- A few degrees higher temperatures in the insulated underlay (B7) during cold periods and in night time, compared to the uninsulated (B4).
- A few degrees higher temperatures in the uninsulated underlay (B4) during day time, and in the summer periods, compared to the insulated underlay (B7).

More plots are available in (Jensen et al., 2019).

Figure 12 show: that the moisture levels for the two attics are rather similar throughout the experimental period. However, the moisture concentration is slightly higher for the insulated underlay during winter, compared to the uninsulated.

[insert Figure 11.]

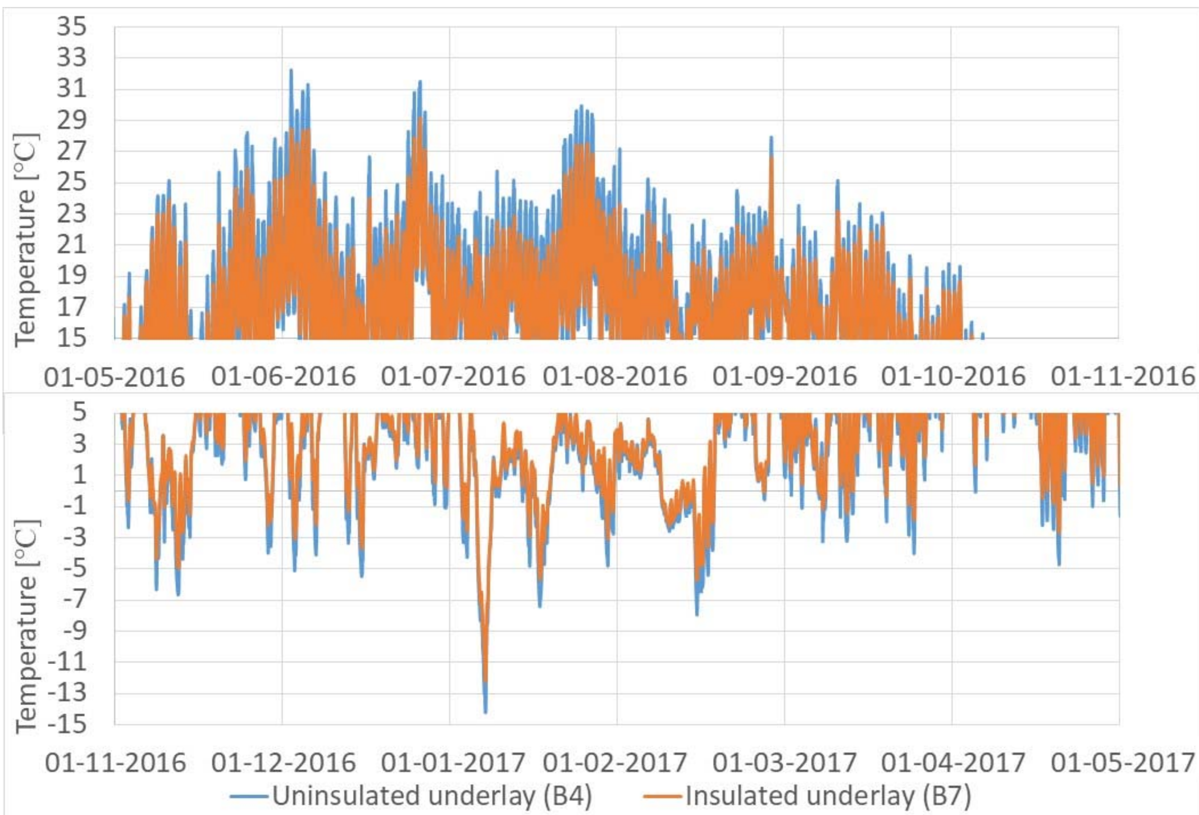

Figure 11 Underlay temperatures measured in underlay with (B7) and without (B4) exterior insulation during the last a) summer period and b) winter period.

[insert Figure 12.]

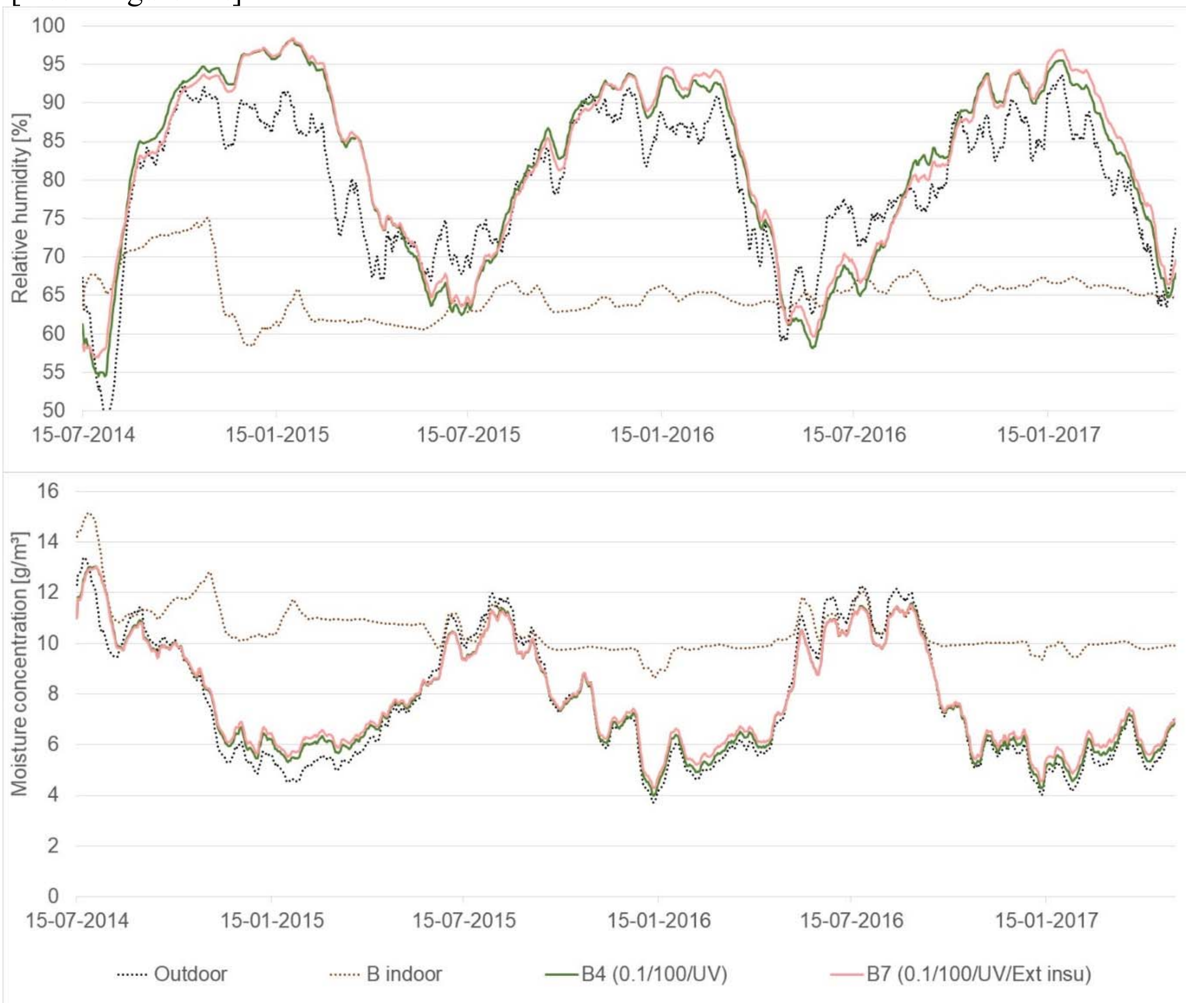

Figure 12 RH (a) and moisture concentration (b) in unventilated diffusion-open attics, comparing attics with and without external roof insulation.

Tracer gas experiment

Table 3**Error! Reference source not found.** presents the Freon 134a gas concentrations, derived infiltration and ventilation airflows for the four attics obtained from pressure and tracer gas measurements. As described in the "Airflows" section, the ventilation airflows were determined mathematically using the mass balances for tracer gas and the mass balances for air (equation 8), and the infiltration flows derived from the pressure measurements (equations 2-7). Table 3 show:

- Ventilation inlet flows are from 20 to 47 % larger than the infiltration flows for the SSV attics, within the period of the tracer gas measurements.
- The diffusion-open attics showed higher infiltration and/or ventilation flows compared to the diffusion-tight attics.

- A comparison of attics A5 and A7 show higher infiltration and ventilation flows with increasing infiltration flow area from 0.00008 m^2 and 0.00014 m^2.

Table 3 Results from pressure and tracer gas measurements, and derived airflows.

Type of result	A5	A7	B5	B6
Freon concentration, indoor [ppm]	8.03	8.13	8.07	8
Freon concentration, attic [ppm]	2.78	3.09	3.7	3.53
Infiltration flow rate [m^3/h]	0.08	0.12	0.92	0.54
Infiltration error ± [m^3/h]	0.05	0.06	0.32	0.32
Ventilation flow rate, in [m^3/h]	0.15	0.19		0.68
Ventilation flow rate, out [m^3/h]	0.24	0.31	2.00	1.22

Mould growth

Mould growth is the result of favourable hygrothermal conditions and available nutrition over time. Performance of individual attics can therefore be assessed by comparison of mould infestation in the attics: Attics with little or no mould growth indicate a good hygrothermal performance, while attics with high mould growth indicate a poor hygrothermal performance. Calculated mould growth was ranked from 0 to 6. For the visual observation, the growth was ranked between 1 and 5, corresponding to no visual growth and heavy growth. Results of the mould modelling and visual observations are shown in Table 4 and Figure 13. Table 4 presents the resulting mould growth index after a period of almost 3 years on 16.05.2017, and visual observations represent the situation 8 months later, on 16.01.2018. Figure 13 shows the development of the mould index as a function of time. The figure serves as a tool to help assess the results for the attics as it summarizes all the presented results.

As the mathematical mould modelling depends highly on the measured RH, but also on the temperature conditions in the attics, analysis results generally follow the same trends as presented in earlier sections. Main observations concerning the modelled risk of mould growth in Figure 13 are presented below:
Increased mould index with increasing diffusion tightness of the underlay for attics without infiltration (B1-3, B9, A1).

Increased infiltration lowers mould index in diffusion-tight unventilated attics (B9, A2, A4, A6), while it increases mould index for diffusion-tight SSV attics (A1, A3, A5, A7).
Increased mould index in diffusion-open attics due to infiltration or ventilation, and an exacerbating effect from combining the two variables (B1-6).
Diffusion-open B8 (Z = 1.0 GPa·s·m^2/kg) performs similar to diffusion-tight A3 (Z = 855 GPa·s·m^2/kg).
Increased mould index in diffusion-tight MV attics with 100 % infiltration compared to unventilated and SSV attics (A9, A2-3). For attics with 20 % infiltration, MV increases mould index compared to SSV attic (A8, A7) but remains below unventilated attic (A6).
A slightly increased mould index in unventilated diffusion-open attics with exterior roof insulation (B7), compared to uninsulated attic (B4).

[insert Figure 13.]

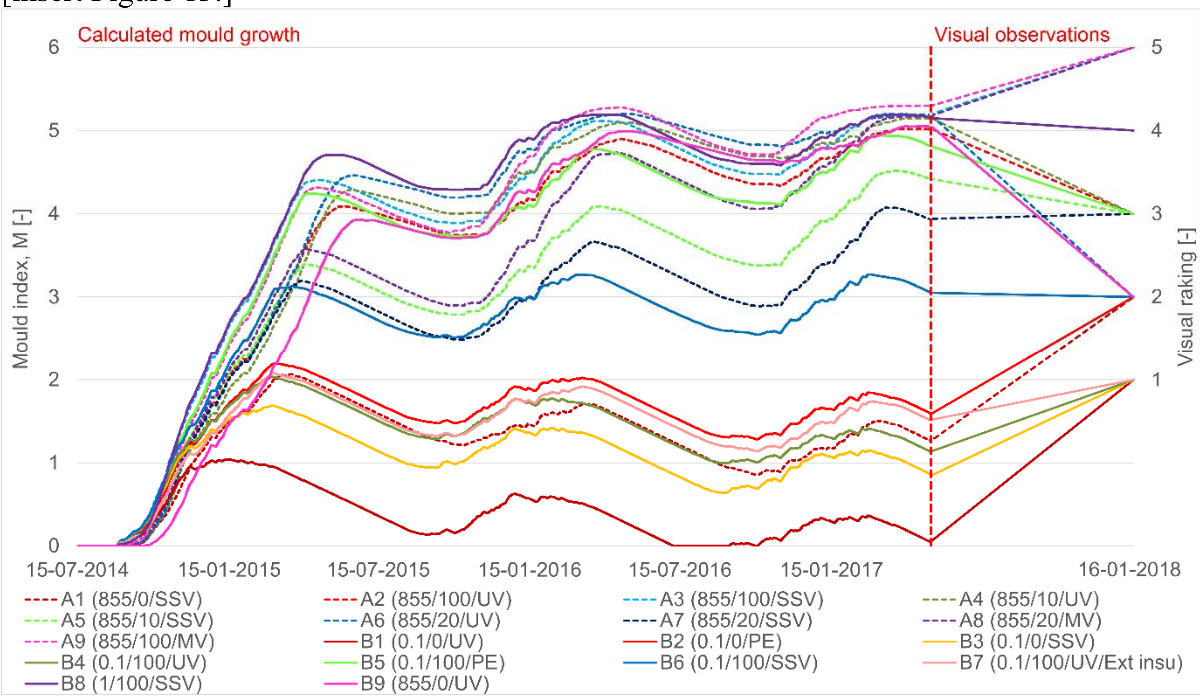

Figure 13 Graphical representation of the calculated mould index as a function of time and the visual ranking for the attics. Note that in the right end of the graph ("Visual observations") the lines connecting the last data points for the calculated mould growth (spring 2017) with the visual ranking 8 months later (January 16th 2018) are only used for graphically showing the relation the two evaluated methods: calculated and observed mould growth. These two scales are not comparable, and therefore there is only a qualitative relation between the calculated and observed mould growth.

Summary of key results

A summary of the key results presented are presented below in Table 4.

Table 4 Summary of key results: mould index, M, after almost 3 years on 16.05.2017, visual observations on 16.01.2018, relative humidity, temperature and moisture concentration.

Attic	Underlay Z-value [GPa·s·m²/kg]	Infiltration [%]	Ventilation strategy [-]	Final VTT model [M]	Visual ranking	Average relative humidity [%]	Standard deviation for relative humidity [%]	Average temperature [°C]	Standard deviation for temperature [°C]	Average moisture concentration [g/m3]	Standard deviation for moisture concentration [g/m3]
A1	855	0	SSV	1.3	2	81.1	13.2	10.0	6.4	7.7	2.0
A2	855	100	UN	5	3	88.7	11.7	10.1	6.3	8.5	2.3
A3	855	100	SSV	5.2	5	87.4	13.6	10.4	6.0	8.4	1.9
A4	855	10	UN	5.1	3	90.0	10.9	10.0	6.3	8.7	2.5
A5	855	10	SSV	4.4	3	85.5	13.5	10.1	6.3	8.1	2.0
A6	855	20	UN	5.2	2	90.7	10.6	10.1	6.3	8.8	2.6
A7	855	20	SSV	3.9	3	84.2	13.9	10.2	6.3	8.0	1.9
A8	855	20	MV	5.2	5	86.0	14.7	10.4	6.3	8.3	1.9
A9	855	100	MV	5.3	5	87.9	14.2	10.6	6.0	8.6	1.9
B1	0.1	0	UN	0	1	79.1	11.0	9.9	6.3	7.6	2.2
B2	0.1	0	PE	1.6	2	82.2	12.3	9.9	6.2	7.8	2.1
B3	0.1	0	SSV	0.9	1	80.8	11.7	9.9	6.2	7.6	2.2
B4	0.1	100	UN	1.1	1	81.9	11.7	9.8	6.2	7.7	2.2
B5	0.1	100	PE	4.8	3	86.6	12.9	10.1	6.0	8.2	2.0
B6	0.1	100	SSV	3	2	84.1	12.3	10.0	6.0	8.0	2.1
B7[1]	0.1	100	UN	1.5	1	82.2	11.4	10.1	5.9	7.9	2.1
B8	1	100	SSV	5.2	4	89.1	12.2	10.0	5.9	8.5	2.0
B9	855	0	UN	5.1	2	90.6	9.3	9.8	6.2	8.6	2.6
A indoor						54.7	2.9	19.5	1.5	9.2	1.1
B indoor						65.1	3.0	18.9	1.5	10.6	1.0
Outdoor						79.5	9.2	9.9	6.2	7.7	2.5

Discussion

Firstly, the performance of the north facing attics under the eaves is accessed according to mould growth level, as presented in Figure 13, followed by interpretation of the results.

Best performance: The best performing attics were all with a diffusion-open underlay and no infiltration, and of those the best performing attic was unventilated. The only attic with 100 % infiltration which had an acceptable performance, had a diffusion-open underlay and no ventilation. Meanwhile, the best performing attic with a diffusion-tight underlay was constructed with SSV and no infiltration.

Average performance: The attics having an average performance were all with SSV. One attic with diffusion-open underlay had 100 % infiltration and SSV, which indicates that SSV worsens the performance compared to no ventilation. Two other attics with diffusion-tight underlay, also with SSV, had 10 % and 20 % infiltration, which indicates that even a relatively small infiltration can have a profound impact on the performance of attics with SSV.

Worst performance: The worst performing attic with a diffusion-open underlay, had 100 % infiltration in combination with PE, indicating that also this ventilation strategy worsens the performance compared to no ventilation.

The worst performing attics with diffusion-tight underlay, were with either 100 % infiltration, no ventilation or mechanical ventilation. The attic with a roofing underlay like phase one, was observed to perform similar to a diffusion-tight underlay in phase two. An attic with mechanical ventilation and diffusion-tight underlay performs even worse than an unventilated attic. For 100 % infiltration, the performance is indicated to be worsened by having mechanical ventilation, as this attic was observed to have the worst mould conditions.

Effect of diffusion tightness of the roofing underlay

For the effect of diffusion tightness of the underlay in cold attic spaces under the eaves without infiltration, relative humidity levels (Figure 3) and risk of mould growth (Figure 13) increases with increasing diffusion resistance of the underlay. Attics similar in design except for the diffusion resistance of the underlay show no rise in temperature (Figure 4), indicate that increased diffusion resistance of the underlay does not change the infiltration air flow from the container to the attic in this experimental setup. The higher moisture levels observed in attics with diffusion-tight underlay compared to diffusion-open is due to the much higher diffusion resistance of the tight underlay, allowing less moisture to leave the attic through the underlay itself.

In addition, the mould risk (Figure 13) increased with increasing diffusion resistance of the roofing underlay also for attics without ventilation (B4 and A2) and with SSV ventilation (B6 and A3), in case of infiltration from the indoor environment.

Findings from (Uvsløkk, 2005) on full sized attics similarly indicate an increased risk of mould growth in attics with increasing diffusion resistance of the underlay, while (Essah et al., 2009) found increased risk of condensation within the attic.

Effect of infiltration in a series of attics with diffusion-open roofing underlay

The worsening of the hygrothermal conditions in diffusion-open cold attic spaces under the eaves due to infiltration, ventilation and the combination (Figure 6 and 14) confirms previous findings within the present project (Bjarløv et al., 2016; Pold, 2015). A leaky ceiling and roof construction seem to allow stack effect to cause an updraft of the infiltration air. The findings that passive ventilation increases moisture levels by allowing for more infiltration are in agreement with (Essah et al., 2009; Harderup and Arfvidsson, 2013; Kalagasidis, 2004; Ojanen, 2001; Samuelson, 1995). However, unlike PH1 (Bjarløv et al., 2016) where the attics with diffusion-open underlay and SSV showed highest moisture levels and mould risk, the present results are in agreement with simulations in (Pold, 2015) showing highest levels for the PE attic. In accordance with the results in (Pold, 2015), the increased moisture levels in the PE attic may be caused by a negative pressure generated in the attic by wind actions which cannot be equalized by outdoor air entering via the lower valve, and therefore must be replaced by infiltrating air. The lack of a lower valve in the PE ventilation strategy further reduces the possibility for equalizing the pressure difference, resulting in an increased replacement by infiltrating air compared to the SSV ventilation strategy. The disagreement with (Bjarløv et al., 2016) concerning the "order of the attics" could be the result of utilizing another type of underlay in PH2 with different diffusion resistance, allowing different quantities of moisture to enter and leave the attic. While there were some small differences between the weather patterns of the two phases, the results are still considered to be useful for comparison.

Effect of infiltration and the influence of roofing underlay airtightness in a series of attics with diffusion-tight roofing underlay

Results from sections "Effect of infiltration in a series of attics with diffusion-tight roofing underlay" and "Effect of infiltration and ventilation" are discussed together in this section to avoid repetition as the same phenomena are involved.

The comparison between unventilated diffusion-tight cold attic spaces under the eaves with different infiltration rates (A2, A4, A6, B9) in Figure 5 and 8 shows reduced relative humidity and moisture concentration during summer with increasing infiltration flow area, while a small increase occurs during winter for the relative humidity. Moisture buffering of the wooden elements could explain this phenomena, as wood releases moisture to the attic air during periods with rising temperatures (Nielsen and Gottfredsen, 1997). For the unventilated diffusion-tight attics without infiltration, moisture released by the wooden elements has no means of escape as it cannot penetrate through the tight underlay, resulting in higher moisture levels during summer. However, with leakages (in this experiment via the intended infiltration tubes, Figure 1) to the indoor environment, moisture can escape downwards, thus lowering moisture levels in the attic. With increasing infiltration flow area, escape to the indoor environment becomes easier, resulting in even lower moisture levels. This leakage situation is considered unfavourable, as it may spread any mould spores and their toxins to the occupied zones. Regarding the risk of mould growth in Figure 13, a slight reduction in risk occurs for the attic with 100 % infiltration (A2) compared to the attic without infiltration (B9). Despite the possibility to leak moisture to occupied zones, attics with 10 and 20 % infiltration (A4, A6) experience an increased risk of mould growth, possibly related to the slightly higher RH during winter.

Opposite to the unventilated diffusion-tight attics, moisture levels increases in the diffusion-tight SSV attics (A1, A3, A5, A7) with increasing infiltration area (Figure 5 and 9). The combination of SSV ventilation and infiltration connects the outdoor and indoor environments, causing worse hygrothermal conditions in the attic, as discussed for diffusion-open attics. Similar is seen for the mould growth risk in Figure 13. Lastly, SSV reduces moisture levels and mould risk for diffusion-tight attics without infiltration (B9, A1) (Figure 5 and Figure 13). SSV also reduces moisture levels for the attics with 10 and 20 % infiltration (A4, A5, A6, A7) (Figure 13). As earlier mentioned, ventilation has a positive effect in cases where moisture is unable to escape downwards from attics with little or no infiltration. This correlate with (Essah et al., 2009), suggesting reduced condensation risk in diffusion-tight attics, with little or no infiltration and eave-to-eave ventilation. The findings with combined ventilation and infiltration are however contradicting (Fugler, 1999; Hagentoft, 2011; Kalagasidis and Mattsson, 2014).

Occurrence of natural ventilation in the attic space under the eaves and performance compared to the mechanical system

The comparison between the diffusion-tight cold attic spaces under the eaves with SSV or MV and 100 % infiltration (A3, A9) (Figure 9 and Figure 13) shows slightly worse hygrothermal conditions in the attic with constant ACH provided by the MV strategy. The two ventilated attics perform better during summer compared to the unventilated attic (A2), but slightly worse in winter. The comparison of moisture levels in the unventilated, SSV and MV attics suggests that natural ventilation does occur for the SSV attics as illustrated in Figure 2b and not the phenomena illustrated in Figure 2c (air passing over the SSV attics). The SSV attics show rather similar tendencies to the MV attics (where the airflow directions are known) throughout the experimental period. In case the phenomena illustrated in Figure 2c was true, moisture levels in the SSV attics would have been considerably higher during winter compared to MV attics as the infiltration rates would be larger due to the low pressure occurring in the air cavity. However, this do not seem to be the case. This is also evident from the temperatures during winter in Figure 10b, where the MV attic shows the highest values, indicating a larger infiltration flow compared to the SSV attic. Meanwhile the unventilated attic shows the lowest temperatures as no air leave the attic through the tight underlay. Airflows determined from the pressure and tracer gas measurements support the results for moisture and temperature, pointing towards the ventilation scenario in Figure 2b, as outside air was shown to enter and leave the attics via the ventilation valves in the underlay (Table 3). With above sets of results, it seems plausible to reason that an airflow scenario similar to Figure 2b occur within the naturally ventilated SSV attics. The

experiment does not provide exact figures for the air entering and leaving the individual valves, however it gives the total for the air inlet and outlet. The findings are in line with the CFD simulations carried out for these SSV attics in (Pold, 2015), showing outdoor air entering the attic from the lower valve and exiting from the upper valve.
Regarding the performance of the SSV attics compared to the MV attics. Findings in previous sections show that increased ventilation leads to higher moisture levels in the attics, the observed higher moisture levels in the MV attics suggest a higher average ACH, and a larger stack effect as a result of this. The higher average ACH in the MV attics could be explained by the combination of a constant airflow (0.22 l/s or 0.79 m3/h) in the MV attics, with occasional peaks from natural ventilation that exceed the constant mechanical airflow. The larger stack effect due to an on average higher ACH, is supported by the temperatures in Figure 10b, showing that the MV attic is warmer during winter compared to the naturally ventilated and unventilated attics. Since the heat can only come from the heated space inside the container during this time of the year, this indicate a higher infiltration caused by stack effect. Studies (Harderup and Arfvidsson, 2013; Holm and Lengsfeld, 2006; Nik et al., 2012; Ojanen, 2001; Pold, 2015) dealing with both diffusion-open and –tight attics support above findings indicating that increased ventilation in the attics causes a rise in the moisture levels, meanwhile (Ge et al., 2018; Roppel and Lawton, 2014) suggests increased ventilation lowers condensation risk and thus contradict present findings. However, as mentioned by (Fugler, 1999; Hagentoft and Kalagasidis, 2008, 2010; Iffa and Tariku, 2016; Roppel and Lawton, 2014; TenWolde and Rose, 1999) the benefit from reduced ventilation may only be true for certain regions. The comparison between the three ventilation scenarios for diffusion-tight attics suggest that some amount of ventilation is necessary, but that high ventilation flows worsen the performance. This is in agreement with (Fugler, 1999; Kalagasidis and Mattsson, 2014; Roppel and Lawton, 2014).

Effect of exterior roof insulation

Results in Figure 11 show that temperatures in the underlay increases by up to 2.5 °C, as the external insulation reduces heat loss by long-wave radiation for the cold attics spaces under the eaves. The average increase is 0.5 °C. The findings correlate with (Harderup and Arfvidsson, 2013). The temperature increase is of importance since the underlay is subject to temperatures several degrees below that of the outdoor air. This represents a potential risk of condensation when the attics are ventilated using outdoor air. (Harderup and Arfvidsson, 2013; Kalagasidis, 2004; Nielsen and Morelli, 2017; Roppel and Lawton, 2014; Samuelson, 1995) have similarly observed lower temperatures in the attic construction compared to the outdoor air during cold periods, with potential risk of condensation. Despite the increased temperature in the underlay, Figure 1213 shows slightly increased moisture concentration and mould growth risk. (Harderup and Arfvidsson, 2013) also observe slightly increased moisture levels in externally insulated attics, while simulations in (Fugler, 1999; Nik et al., 2012) indicated improved performance. All studies did however experience damaging moisture levels despite the external roof insulation, which also correlate with present findings.

Calculated and visual mould observations

With a few exceptions, a good agreement is seen between the visual mould observations and calculated mould growth in Figure 13. Most diffusion-open attics show no or weak mould growth, while the diffusion-tight attics show visible or heavy mould growth. Most notable exceptions are the unventilated diffusion-tight attics with 0 % and 20 % infiltration (B9, A6). Despite showing high RH throughout the experimental period and a calculated mould index above 5, the visual mould observations showed little mould growth in the attics. However, these two attics (and possibly others), could have more mould infestation than indicated by the visual observations, since some growth may not be visible to the naked eye. The lack of visual mould in these attics could be caused by the different colour pigment of the mould species growing in these attics, lack of certain nutrients from the substrate, or due to the current growth phase of the mould as described in (Eagen et al., 1997; Fleet et al., 2001; Gadd, 1980; Johansson et al., 2014). These observations are in line with results from the previous mould registration within the project (Pold, 2015), in which visual observations, air samples and swab tests were compared for several attics. Results showed inconsistency between visual observation and the two other methods, including samples taken from attic A6. Therefore, visual observations should be complemented by other quantitative methods accounting for non-visual mould growth such as the Mycometer® surface test (Krause, 2003; Mycometer, 2012; Reeslev and Miller, 2000; Schrock et al., 2011) measuring the fluorescent product released from the enzyme substrate complex which relate to the N-acetylhexosaminidase activity found in mould. Also, samples could be inspected for microscopic fungal growth at 40 times magnification and ranked accordingly, as described in (Johansson et al., 2014). Yet another uncertainty for the comparison between rankings is that the visual mould observation was performed eight months after the last data point used for the mathematical model, which may have offset the results of several attics.

General for the experimental setup

Results presented in this paper are for cold attics spaces under the eaves in a cool temperate climate, located adjacent to an occupied zone with 20 °C and RH of 60 % throughout the year. Furthermore, while the 60 % indoor RH is fitting for summer conditions, it might be too high for winter conditions. Levels between 30 and 50 % are suggested by (Brandt et al., 2013) in winter, which are likely to impact the hygrothermal performance of the attics. The physical location of the individual attic was another general uncertainty, since it was theorized that wind conditions would be different around attics located in the centre of the experimental setup compared to attics at the ends of container A or B. However, no systematic tendencies were observed which could be explained by the physical location of the individual attics. More data on local wind conditions would have been valuable in reaching a better understanding of the results in relation to the physical location of the individual attics. Regarding comparison between attics in container A or B; some differences were observed between the two indoor climates. However, no comparison was made between container A or B for attics with infiltration, thus the differences in the indoor climates should not be of great importance.

Measurement uncertainties would primarily be an issue at high relative humidity values where uncertainty of the equipment is at its largest. Looking at the comparisons presented in the results section, measurement uncertainties would mainly influence the results for some of the worse performing attics with diffusion-tight roofing underlay. Some of these attics have periods of several months with relative humidity values around 98-100 %. Meanwhile, the attics with diffusion-open roofing underlay (and the diffusion-tight A1) do however maintain levels below 95 % for the majority of the experimental period. Hence, the more overall conclusion regarding what are the best and worst performing attics will not change due to minor measurement uncertainties.

Conclusions

This paper presents the results from a large-scale experimental setup investigating the hygrothermal performance of 18 north facing cold attic spaces under the eaves in a cool temperate climate, for almost 3 years. Different measures to tackle the problem of unfavourable moisture conditions in cold attic spaces under the eaves were combined and studied. These included varying the underlay, ventilation strategy, infiltration rate and externally insulated underlay as parameters. Relative humidity and temperature were measured continuously at multiple locations throughout the experimental setup. The objective was to test best practice recommendations according to Danish guidelines (Brandt et al., 2009, 2013) for design of cold attic spaces under the eaves, and to comply with the requirements for airtightness of the building envelope according to (TBST, 2018).

Main findings are:

Compliance with the Danish building regulations 2018 (BR18) (TBST, 2018) for airtightness of the building envelope (less than 1.0 l/s per m^2 heated floor area at 50 Pa pressure difference) and best practice guidelines does not ensure satisfactory moisture levels in north facing attic spaces under the eaves, in order to prevent mould growth.

The hygrothermal performance of north facing attic spaces under the eaves is worsened with increasing vapour diffusion tightness of the underlay. With no observed change in the leakage air flow passing through the attic as an effect of altered diffusion tightness, the worsened performance is likely due to increased diffusion resistance. This indicates that the lower the diffusion tightness of the underlay the better.

Single-sided ventilation and pressure equalization as according to Danish guidelines (Brandt et al., 2009, 2013) worsens the hygrothermal performance of north oriented attic spaces under the eaves with diffusion-open underlay.

Pressure equalization resulted in the worst hygrothermal performance in the north oriented attic spaces under the eaves with diffusion-open underlay in this study, while results in a previous study (Bjarløv et al., 2016)indicated worst performance for single-sided ventilation.

For north oriented attic spaces under the eaves with diffusion-tight underlay, the best performance was seen for attic with single-sided ventilation and no infiltration. With increasing infiltration area the hygrothermal performance was worsened.

Natural ventilation does occur within the cold attic spaces under the eaves. It was found that air in the ventilated cavity entered the attic spaces and did not bypass the valves entirely.
Ventilation of attic with diffusion-tight underlay is necessary. However, too much ventilation seem to worsen the conditions. A smaller sized ventilation valve (flow area < 50 cm^2) may improve the performance of the naturally ventilated attics.
External roof insulation reduced heat loss due to long-wave radiation, this increased the temperature in the underlay and lowered the risk of condensation on the internal surface of the roofing underlay. The external insulation did however not improve the overall hygrothermal performance significantly in the studied case. More data and analysis regarding various design scenarios with externally insulated underlay are therefore needed to draw more general conclusions on this issue.
There was a good agreement between predicted and observed mould growth in the studied attics. The results of this study indicate that post processing hygrothermal measurements with a mould growth model gives a good prediction of the real performance. Divergences between these two methods may rely on the fact that a portion of the mould infestation was unnoticed, because only visual observations were performed.

Conflict of interest

The authors confirm that there are no known conflicts of interest associated with this publication, and there has been no financial support for this work that could have influenced its outcome.

References

Bjarløv SP, Johnston CJ and Hansen MH (2016) Hygrothermal conditions in cold, north facing attic spaces under the eaves with vapour-open roofing underlay in a cool, temperate climate. *Building and Environment* 95. Elsevier Ltd: 272–282. DOI: 10.1016/j.buildenv.2015.09.009.

Boverket (2009) *BETSI main report 'Så mår våra hus' (Swedish)*. Karlskrona, Sweden.

Brandt E, Bunch-Nielsen T, Christensen G, et al. (2009) *SBi-Anvisning 224 - Fugt i Bygninger (Danish)*. 1st ed. Hørsholm, Denmark: Statens Byggeforskningensinstitut, Aalborg University.

Brandt E, Bunch-Nielsen T, Christensen G, et al. (2013) *SBi-Anvisning 224 - Fugt i Bygninger (Danish)*. 2nd ed. Hørsholm, Denmark: Statens Byggeforskningensinstitut, Aalborg University.

Brischke C and Thelandersson S (2014) Modelling the outdoor performance of wood products - A review on existing approaches. *Construction and Building Materials* 66. Elsevier Ltd: 384–397. DOI: 10.1016/j.conbuildmat.2014.05.087.

DS/EN ISO 13788 (2013) Hygrothermal performance of building components and building elements. Internal surface temperature to avoid critical surface humidity and interstitial condensation. Calculation methods, 2. edition. Charlottenlund,

Denmark: Dansk Standard/Danish Standards.
Eagen R, Brisson A and Breuil C (1997) The sap-staining fungus Ophiostoma piceae synthesizes different types of melanin in different growth media. *Canadian Journal of Microbiology* 43(6): 592–595. DOI: 10.1139/m97-084.
Essah EA, Sanders CH, Baker P, et al. (2009) Condensation and moisture transport in cold roofs: Effects of roof underlay. *Building Research and Information* 37(2): 117–128. DOI: 10.1080/09613210802645973.
Fleet C, Breuil C and Uzunovic A (2001) Nutrient consumption and pigmentation of deep and surface colonizing sapstaining fungi in Pinus contorta. *Holzforschung* 55(4): 340–346. DOI: 10.1515/HF.2001.057.
Fugler DW (1999) Conclusions from ten years of Canadian attic research. *ASHRAE Transactions*.
Gadd GM (1980) Melanin production and differentiation in batch cultures of the polymorphic fungus Aureobasidium pullulans. *FEMS Microbiology Letters* 9(3): 237–240. DOI: doi:10.1016/0378-1097(80)90132-9.
Ge H, Wang R and Baril D (2018) Field measurements of hygrothermal performance of attics in extreme cold climates. *Building and Environment* 134(November 2017). Elsevier: 114–130. DOI: 10.1016/j.buildenv.2018.02.032.
Gradeci K, Labonnote N, Time B, et al. (2017) Mould growth criteria and design avoidance approaches in wood-based materials – A systematic review. *Construction and Building Materials* 150. Elsevier Ltd: 77–88. DOI: 10.1016/j.conbuildmat.2017.05.204.
Gradeci K, Labonnote N, Köhler J, et al. (2017) Mould Models Applicable to Wood-Based Materials-A Generic Framework. *Energy Procedia* 132. Elsevier B.V.: 177–182. DOI: 10.1016/j.egypro.2017.09.751.
Hagentoft, Carl-eric; Kalagasidis AS (2013) Hygrothermal Conditions and Mould Growth Potential in Cold Attics: Impact of Weather, Building System and Construction Design Characteristics in Building Pathology and Rehabilitation. In: *Journal of Building Pathology and Rehabilitation*, 2013, pp. 61–91. DOI: DOI 10.1007/978-3-642-31158-1.
Hagentoft C-E (2011) Probabilistic analysis of hygrothermal conditions and mould growth potential in cold attics. Impact of weather parameters, building systems and construction design characteristics. In: *Proceedings of the 12DBMC - International Conference on Durability of Building Materials and Components*, Porto, Portugal, 2011, pp. 1–8. in-house publishing.
Hagentoft C and Kalagasidis AS (2008) Mould growth control in cold attics through adaptive ventilation. In: *Proceedings of the 8th symposium on building physics in the nordic countries*, Copenhagen, Denmark, 2008.
Hagentoft C and Kalagasidis AS (2010) Mold Growth Control in Cold Attics through Adaptive Ventilation: Validation by Field Measurements. In: *11th International Conference on Thermal Performance of the Exterior Envelopes of Whole Buildings, Buildings XI*, Clearwater Beach, Florida, US, 2010.
Hagentoft C and Kalagasidis AS (2014) Moisture safe cold attics - Assessmentt based on risk analyses of performance and cost. In: *Proceedings of the 10th Nordic Symposium on Building Physics*, 2014, pp. 1366–1373.
Hagentoft CE and Kalagasidis AS (2016) Drying Potential of Cold Attic Using Natural

and Controlled Ventilation in Different Swedish Climates. In: *Procedia Engineering*, 2016, pp. 2–7. Elsevier B.V. DOI: 10.1016/j.proeng.2016.06.345.
Harderup L-E and Arfvidsson J (2013) Moisture safety in cold attics with thick thermal insulation. *Journal of Architectural Engineering* 19: 265–278.
Holm A and Lengsfeld K (2006) Hygrothermal performance of unfinished attics (ventilated roofs) - an experimental study. In: *Proceedings of the 3rd International Conference in Building Physics - Research in Building Physics and Building Engineering*, Montreal, Canada, 2006, pp. 451–457. Pr Mgr Eng. Taylor & Francis LTD.
Hukka A and Viitanen HA (1999) A mathematical model of mould growth on wooden material. *Wood Science and Technology* 33(6): 475–485. DOI: 10.1007/s002260050131.
Iffa E and Tariku F (2016) Hygrothermal performance of ventilated attic in marine climate under different ceiling air tightness. In: *Indoor Air Journal*, Ghent, Belgium, 2016, pp. 1–8. Available at: https://www.isiaq.org/docs/Papers/Paper1141.pdf.
Isaksson T, Thelandersson S, Ekstrand-Tobin A, et al. (2010) Critical conditions for onset of mould growth under varying climate conditions. *Building and Environment* 45(7). Elsevier Ltd: 1712–1721. DOI: 10.1016/j.buildenv.2010.01.023.
Jensen NF, Bjarløv SP, Johnston CJ, et al. (2019) Hygrothermal assessment of north facing, cold attic spaces under the eaves with varying structural roof scenarios. Available at: http://orbit.dtu.dk/en/projects/hygrothermal-assessment-of-north-facing-cold-attic-spaces-under-the-eaves-with-varying-structural-roof-scenarios(cfdaf1a4-79a3-48f4-98ed-d16d624ea024).html (accessed 23 May 2019).
Johansson P, Ekstrand-Tobin A and Bok G (2014) An innovative test method for evaluating the critical moisture level for mould growth on building materials. *Building and Environment* 81. Elsevier Ltd: 404–409. DOI: 10.1016/j.buildenv.2014.07.002.
Kalagasidis AS (2004) The whole model validation for HAM-Tools. Case study: hygrothermal conditions in the cold attic under different ventilation regimes. *Proceedings of the ASHRAE/DOE/BTECC Conference on the Performance of the Exterior Envelopes of Whole Buildings IX* (Sasic): 1–17.
Kalagasidis AS (2007) Simulations as the Way of Bridging the Gaps between Desired and Actual Hygrothermal Performance of Buildings. *IBPSA 2007 - International Building Performance Simulation Association 2007* (June): 1712–1719. Available at: http://www.scopus.com/inward/record.url?eid=2-s2.0-84869753403&partnerID=tZOtx3y1.
Kalagasidis AS and Mattsson B (2014) MODELLING OF MOISTURE CONDITIONS IN A MODELLING OF MOISTURE CONDITIONS IN A. In: *Ventilation in Relation to the Energy Performance of Buildings: 26th AIVC Conference : Proceedings*, Brussels, Belgium, 2014. Air Infiltration and Ventilation Centre, 2005.
Krause JD (2003) Analytical Instrument Performance Criteria Application: Application of a Fluorometric Method for the Detection of Mold in Indoor Environments. *Applied occupational and environmental hygiene* 18(7): 1–5. DOI: 10.1080/10473220301457.
LumaSense Technologies (2004) INNOVA Product Data 1312 Photoacoustic Multi-gas Monitor. Available at:

https://innova.lumasenseinc.com/784125/?reference=1126&code=8d2340f88c8e46f8637438096ffb4c3b.
Møller EB, Andersen B, Rode C, et al. (2017) Conditions for mould growth on typical interior surfaces. *Energy Procedia* 132. Elsevier B.V.: 171–176. DOI: 10.1016/j.egypro.2017.09.680.
Mycometer (2012) mycometer surface: On-site fungal contamination assessment. Available at: http://cdn.mycometer.com/fileadmin/user_upload/Pdf/Mycometer-Surface_Flyer__2012_.pdf.
Nielsen A and Gottfredsen FR (1997) *Bygningsmaterialer - Grundlæggende Egenskaber (Danish)*. 7th ed. Lyngby, Denmark: Polyteknisk Forlag.
Nielsen A and Morelli M (2017) Measured temperature and moisture conditions in the roof attic of a one-and-a-half story house. *Energy Procedia* 132. Elsevier B.V.: 789–794. DOI: 10.1016/j.egypro.2017.10.028.
Nik VM, Kalagasidis AS and Kjellström E (2012) Assessment of hygrothermal performance and mould growth risk in ventilated attics in respect to possible climate changes in Sweden. *Building and Environment* 55. Elsevier Ltd: 96–109. DOI: 10.1016/j.buildenv.2012.01.024.
Ojanen T, Viitanen H and Peuhkuri R (2007) MODELLING OF MOULD GROWTH IN BUILDING - EXISTING MODELS, DISCUSSION ON IMPROVEMENT ASPETS, SENSIBILITY ANALYSIS. In: *Proceedings of the IEA ECBCS Annex 41 Closing Seminar* (ed. C Rode), Copenhagen, Denmark, 2007, pp. 117–128. Dept. of Civil Engineering, BYG R-191, Technical University of Denmark, Kgs. Lyngby, Denmark. Available at: http://orbit.dtu.dk/files/3156657/byg-r191.pdf.
Ojanen T, Viitanen H, Peuhkuri R, et al. (2010) Mold Growth Modeling of Building Structures Using Sensitivity Classes of Materials. *Thermal Performance of the Exterior Envelopes of Buildings XI*: 1–10. DOI: 10.1081/E-EEE2-120046011.
Ojanen TT (2001) Thermal and Moisture Performance of a Sealed Cold-Roof System with a Vapor-Permeable Underlay. *Thermal Performance of the Exterior Envelopes of Buildings VIII Conference*.
Pold CFH (2015) *Ventilation Design of Cold Attics for Avoiding Moisture-Related Problems*. MSc theis, Department of Civil Engineering, Technical University of Denmark.
Reeslev M and Miller M (2000) The MycoMeter-test. A new rapid method for detection and quantification of mold in buildings. *Proceedings of healthy buildings* 1: 589–590.
Roppel P and Lawton M (2014) *Attic Ventilation and Moisture Research Study - Final Report*. DOI: 10.1002/2014GB005021.
Roppel P, Norris N and Lawton M (2013) Highly insulated, ventilated, wood-framed attics in cool marine climates. In: *Thermal Performance of the Exterior Envelopes of Whole Buildings XII International Conference*, Clearwater, Florida, USA, 2013, pp. 389–401. American Society of Heating, Refrigeration, and Air-Conditioning Engineers (ASHRAE).
Samuelson I (1995) *Moisture balance in Unheated Roof Spaces: The importance of Ventilation and Choice of Insulation Materials. SP rapport 1995:68 (Swedish)*. Borås, Sweden.
Schrock M, Riffle C, Dindal A, et al. (2011) *Environmental Technology Verification*

Report: Mycometer ®-test Rapid Fungi Detection and Bactiquant ®-test Rapid Bacteria Detection Technologies.
Sensirion (2013) Sensirion Differential Pressure SDP1000/SDP2000 datasheet version 5. Available at: http://www.mouser.com/ds/2/682/Sensirion_Differential_Pressure_SDP1000_SDP2000_Da-469650.pdf.
TBST (2018) Danish Building Regulations 2018. Denmark. Available at: http://bygningsreglementet.dk/.
TenWolde A and Rose WB (1999) Issues related to venting of attics and cathedral ceilings. *ASHRAE Transactions* 105, Pt. 1.
Uvsløkk S (2005) Moisture and temperature conditions in cold lofts and risk of mould growth. *Proceedings of the 7th Symposium on Building Physics in the Nordic Countries*: 8.
Viitanen H, Krus M, Ojanen T, et al. (2015) Mold risk classification based on comparative evaluation of two established growth models. *Energy Procedia* 78. Elsevier B.V.: 1425–1430. DOI: 10.1016/j.egypro.2015.11.165.